Pre-dauer starvation decouples somatic from germline development with lifelong reproductive consequences in *C. elegans*

Fred A. Koitz[1], Camille P. Miller[1], Kacy Lynn Gordon[1,2]

[1]Department of Biology, The University of North Carolina at Chapel Hill, Chapel Hill, North Carolina 27599

[2]To whom correspondence should be addressed, kacy.gordon@unc.edu

Running title: Starvation and reproduction

Keywords: *C. elegans,* dauer, starvation, LAG-2, germline, germline stem cell niche

ABSTRACT

Early life stresses impact reproductive outcomes in many organisms. In response to crowding and starvation, *C. elegans* nematodes form dauer larvae, in which development arrests until conditions improve. We discovered dramatic differences in gonad size and germ cell number among dauers that form under different conditions. We used live cell imaging of fluorescent markers in otherwise wild-type and mutant animals combined with food-removal, recovery, and brood-size assays to investigate the causes and consequences of this germline difference. Pre-dauer feeding, but not nutrient sensing via the DAF-2/insulin-like signaling receptor or DAF-7/TGF-β, is required for plasticity in gonad size. Gonad differences in dauer have lifelong reproductive consequences; worms with small dauer gonads recover to have smaller broods. Somatic and germline development are decoupled as pre-dauer starvation induces germline quiescence while the soma continues its development until dauer is formed. A rapid return to germline Notch-dependence and an increase in presentation by the germline stem cell niche of the Notch ligand LAG-2–regulated at the protein and not transcript level–are among the earliest events of dauer recovery.

SUMMARY STATEMENT

Pre-dauer starvation limits the size of the dauer gonad, reduces presentation of the germline niche cue LAG-2, and diminishes future reproductive success.

INTRODUCTION

Lifelong development requires environmental responsiveness within the developmental program. A special case of developmental response to difficult environmental conditions is the diapause state, in which development arrests in unfavorable conditions and resumes when conditions improve (Harsimran Kaur Gill et al., 2017; Renfree and Fenelon, 2017). While diapause states can be obligate - that is, built into an animal's life cycle in anticipation of poor conditions - other diapause states are facultative and responsive to an organism's present environment (Hand et al., 2016; Wilsterman et al., 2021). One well-studied facultative diapause state is the *C. elegans* dauer (Cassada and Russell, 1975), formed in response to starvation and crowding sensed by pheromone (Golden and Riddle, 1984a) and enhanced by higher temperatures (Ailion and Thomas, 2000). Dauer larvae withstand poor environmental conditions (Cassada and Russell, 1975; Golden and Riddle, 1984a) for many times the typical lifespan of a worm (Klass and Hirsh, 1976). Improved environmental conditions trigger exit from dauer, resumption of development, and a (mostly) normal reproductive life (Cassada and Russell, 1975; Klass and Hirsh, 1976). Famously, time spent in the dauer larval stage does not affect adult lifespan (Klass and Hirsh, 1976).

It is the preservation of fertility rather than increased lifespan alone that makes dauer adaptive (Schluter et al., 1991). Previous studies disagree about the long-term effects of dauer for future reproduction (Kim and Paik, 2008; Klass and Hirsh, 1976; Ow et al., 2018; Webster et al., 2018). These studies focused on recovery and did not investigate differences of the cells of the dauer reproductive system itself. We set out to investigate the cells of the gonad and germline during the dauer larval period to look for developmental antecedents of later reproductive differences.

To introduce our study, we present brief summaries of the parallel processes of the dauer decision and early reproductive system development. The *C. elegans* life cycle goes from embryonic development through four larval stages (L1-L4) punctuated by molting before a terminal molt into the adult reproductive form (Corsi et al., 2015). The dauer is an alternate third larval stage. Entry into the dauer developmental pathway is specified in the first larval stage (L1) and is followed by a second stage called L2d (Golden and Riddle, 1984a). In persistently harsh conditions, the L2d molts into a dauer larva with a thick cuticle, arrested development, and altered metabolism (Cassada and Russell, 1975; Erkut and Kurzchalia, 2015; Golden and Riddle, 1984a; Wadsworth and Riddle, 1989).

The *C. elegans* hermaphrodite reproductive system develops post-embryonically from a 4-cell primordium of two somatic blast cells and two primordial germ cells (Kimble and Hirsh, 1979). In the L1 stage, a germline stem cell niche, the distal tip cell (DTC) is born from each of the somatic blast cells and the primordial germ cells make a first division or two in the L1 larval stage (Kimble and Hirsh, 1979). The germline relies on DTC expression of the stemness cue LAG-2, a Delta/Serrate/LAG-2 (DSL) ligand of the Notch signaling pathway to maintain germ cells in an undifferentiated state throughout development (Kimble and Crittenden, 2005). By the end of the L2 stage a population of 20-30 germ cells (Kimble and White, 1981) is supported by two DTCs and a 10-cell somatic gonad primordium (Kimble and Hirsh, 1979). The developmental arrest of gonad and germ cell lineages in the dauer larva have been investigated genetically (Narbonne and Roy, 2006; Tenen and Greenwald, 2019), primarily using genetic mutants that constitutively form dauers at high temperature.

Among these are mutations to genes in the insulin-IGF-1 signaling (IIS) pathway, including the gene encoding the sole *C. elegans* IIS receptor *daf-2* (Kimura et al., 1997). IIS integrates nutritional status with metabolism, developmental control, reproduction, and aging in *C. elegans* (Murphy and Hu, 2013) and in other organisms, including humans (Barbieri et al., 2003; Claeys et al., 2002; Das and Arur, 2017). A reduction-of-function allele, *daf-2(e1370),* is commonly used to induce dauer larvae at high temperature in experimental settings (Karp, 2018). Another reduction-of-function allele, *daf-7(e1372)*, affecting a parallel pathway leading to dauer entry–TGF-β signaling–also forms dauers constitutively at high temperature (Karp, 2018). The TGF-β pathway links external cues to the reproductive system (Dalfó et al., 2012; Pekar et al., 2017). The germline is especially sensitive to starvation throughout life (Angelo and Van Gilst, 2009; Dalfó et al., 2012; Pekar et al., 2017; Seidel and Kimble, 2011; Webster et al., 2022), so we hypothesized that pre-dauer nutrition may cause differences in the dauer reproductive system that impact post-dauer recovery of fertility.

We discovered that *C. elegans* enter dauer with different numbers of germline cells depending on feeding prior to dauer entry. The most severely starved worms have many times fewer cells and roughly half the brood size upon recovery compared to those that fed the most during pre-dauer development. Surprisingly, the DAF-2/IIS receptor is dispensable for this difference, suggesting that the fed state itself, rather than nutrient sensing via IIS, regulates pre-dauer germline growth. Because the somatic lineage is invariant in *C. elegans* (Kimble and Hirsh, 1979; Sulston and Horvitz, 1977; Sulston et al., 1983), early life starvation decouples germline from somatic development, pausing germline development while the soma continues to the “safe

112 harbor” state of dauer diapause. The mechanism of this decoupling involves reduced
113 presentation of the stemness cue LAG-2 by the germline stem cell niche and the
114 induction of a Notch-independent quiescent state of the germline. This state is rapidly
115 reversed in the DTC and germline upon removal from dauer-forming conditions, and
116 appears to be regulated post-translationally. Altogether, this work reports heretofore
117 unrecognized differences in dauer gonads mediated by pre-dauer nutrient stress effects
118 on niche and stem cell maintenance that predict differential reproductive recovery from
119 dauer.
120
121 **RESULTS**
122 **Dauers that form constitutively have longer gonads than those that form after**
123 **progressive crowding and starvation**
124
125 We examined the gonad in dauer animals under two dauer-induction regimes that are
126 commonly used in the field–facultative dauer entry after starvation and crowding and
127 constitutive dauer forming mutants (Karp, 2018). First, we progressively starved
128 crowded worm growth plates (see Methods) and assayed both “early dauers” on such a
129 plate within the first week of starvation, as well as “late dauers” that were recovered
130 after >4 weeks. We used otherwise wild-type worms expressing markers of the germline
131 (*mex-5p::H2B::mCherry::nos-2 3’UTR*, (Linden et al., 2017)) and an endogenously
132 tagged integrin alpha subunit *ina-1(qy23[ina-1::mNG])*(Jayadev et al., 2019)) that aids
133 visualization of the somatic gonad.
134
135 We also used the field-standard dauer-formation constitutive (daf-c) mutants carrying
136 reduction-of-function alleles of *daf-2(e1370)* and *daf-7(e1372)*, which enter dauer
137 constitutively at high temperature (Karp, 2018). It is thought that DAF-2/IGFR (insulin-
138 like growth factor receptor) or DAF-7/TGF-β function is impaired, respectively, at all
139 rearing temperatures, as non-dauer-related loss-of-function phenotypes are observed at
140 both low and high temperatures (Blackwell et al., 2015; Gems et al., 1998; Greer et al.,
141 2008; Kenyon et al., 1993; McGehee, 2019; Trent et al., 1983; Tullet et al., 2008).
142 Indeed, dauer itself is triggered by high-temperature rearing in wild-type worms (Ailion
143 and Thomas, 2000), so these daf-c mutants are considered to be reduction-of-function
144 alleles that are sensitized for dauer formation at a higher temperature (Golden and
145 Riddle, 1984b).
146
147 This experimental regimen allowed us to compare between early and late dauers,
148 among genotypes after progressive starvation (control with gonad fluorescent markers
149 compared to *daf-2(e1370)* and *daf-7(e1372)*), and between modes of dauer induction
150 for both mutant genotypes (progressive starvation vs. constitutive entry, for both early
151 and late dauers).

Under progressive starvation, early dauers of all three genotypes had longer gonads than late dauers, by nearly 2x on average (Fig. 1A,B). This raised the possibility that dauer gonads change over time. We tested this hypothesis by using the dauer constitutive mutants to form a population of constitutive, synchronous dauers and measuring both early and late dauers for gonad size. Neither mutant showed a time-related change of gonad length over a month in dauer (Fig. 1C,D), suggesting that time spent in dauer was not responsible for the smaller gonads seen in control late dauers. We therefore concluded that neither genotype (*daf-2(e1370)* or *daf-7(e1372)* vs. control) nor time in dauer (over one month) is responsible for the gonad size difference between early and late dauers formed by progressive starvation.

Worms with longer gonads have better post-dauer reproductive recovery than worms with shorter gonads, regardless of genotype

We next asked if these same dauer-forming conditions for the same genotypes considered above had functional consequences for post-dauer reproductive success. We recovered dauers (Methods) and tracked individual worm recovery and eventual brood size (Fig. 1E). For each genotype, we included a never-dauer, continuously-fed control, since brood size can vary across strains. Otherwise wild-type worms with fluorescent markers (see next section) show a normal brood size (of ~244 ± 31) in never-dauer controls. Early dauers induced by progressive starvation (which have long gonads, Fig. 1A) recover to produce a normal brood (271 ± 47) (Fig. 1F Early). In contrast, late dauers (which have small gonads, Fig. 1A) recover to produce a substantially decreased brood size compared to the early dauers (171 ± 112) (Fig. 1F Late). The same pattern is observed for the *daf-2(e1370)* mutant genotype after progressive starvation: early dauers (long gonads, Fig. 1A,B) produce normal broods relative to the never-dauer control, while late dauers (short gonads, Fig. 1C,D) have worse reproductive recovery (Fig. 1G).

When mutant *daf-2(e1370)* animals with the germ cell nuclear marker constitutively entered dauer (larger germlines, Fig. 1C,D) both early and late dauers recovered equally well, both producing broods equivalent to the never-dauer control of that genotype (Fig.1G). Therefore, time spent in dauer alone did not reduce the brood of subsequently recovered dauer animals. From these brood size assays, we concluded that dauer gonad size was best correlated with post-dauer reproductive success. We next asked what determines dauer gonad size.

Two of our prior experiments and one published finding (Cassada and Russell, 1975) implicate pre-dauer feeding as a potential determinant of gonad size in dauer. First,

192 when we used daf-c alleles to induce constitutive dauer formation at high temperature,
193 the worms feed continuously until right before dauer entry and had uniformly large
194 gonads and brood. Second, for all genotypes exposed to progressive starvation, early
195 dauers from newly starved plates had large gonads and broods, and may have had
196 access to more food during pre-dauer development than late dauers. Finally, dauer
197 body length differs proportionally with the titre of bacterial food that worms ate prior to
198 dauer (Cassada and Russell, 1975). We hypothesized that pre-dauer feeding
199 determines gonad size in dauer.
200
201 **Starvation in the second larval stage decouples germline development from**
202 **somatic development independent of insulin-like signaling**
203
204 To test the hypothesis that feeding is responsible for dauer gonad length, we
205 manipulated *daf-2(e1370)* daf-c mutants expressing a germ cell nuclear marker (*mex-*
206 *5p::H2B::mCherry::nos-2 3'UTR*, (Linden et al., 2017)) in a series of food removal
207 experiments. The use of a daf-c mutant at 25°C ensured that we could vary food
208 exposure while ensuring every animal was in the L2d dauer entry program. Worms were
209 reared on growth plates with a lawn of bacterial food for the specified number of hours
210 at 25°C (Fig. 2A), removed from food at 25°C, and maintained until the endpoint at
211 which a population of majority dauers was noted.
212
213 We assayed germ cell number directly upon removal from food and again within a day
214 of dauer entry to test the relationship between time spent feeding and germ cell number,
215 and how much germ cell number changed between the cessation of feeding and entry
216 into dauer (Fig. 2B). We found a proportional relationship between time spent feeding
217 and germ cell number at the time of food removal and in dauer.
218
219 Between removal from food at the 12, 16, and 20 hours fed timepoints, it appears that
220 cells undergo one additional round of division before dauer entry (average germ cell
221 numbers approximately double, Fig. 2B,C). After 24 hours or longer of L2d feeding, the
222 increase in cell number before dauer entry is less dramatic, likely reflecting that late L2d
223 animals begin to slow germ cell division in preparation for dauer entry ((Narbonne and
224 Roy, 2006), also in *daf-2(e1370)* mutants). Germ cells will complete an average of one
225 additional cell division after DTC laser ablation in the L2-L3 stages of development
226 (Kimble and White, 1981), and genetic ablation of the stemness receptor GLP-1/Notch
227 allows germ cells to complete their current mitotic cell cycle and make a terminal
228 division before differentiating (Fox and Schedl, 2015). Our finding that germ cells
229 complete one round of division after food removal (Fig. 2B,D) tracks with our
230 established understanding of cell cycle constraints on stem-like germ cell proliferative
231 dynamics.

Comparing the rate of germline growth among these treatments revealed an even more dramatic response to starvation than that of germ cell number alone (Fig. 2D). Animals that fed (12h fed+24h fed) gained an average of about one germ cell per hour, while animals that starved (12h fed+24h starved) added only one germ cell in that 24 hour period (Fig. 2D, gray shaded box). In response to starvation, animals are able to arrest germline development while slowing but not arresting somatic development until the dauer larva is formed (Fig. 2E and (Cassada and Russell, 1975)), demonstrating a decoupling of germline development from somatic development during the L2d period. Because these experiments were done in *daf-2(e1370)* mutants, another major conclusion from this experiment is that DAF-2/IGFR-mediated nutrient sensing itself is not required for worms to modulate gonad size in response to food removal.

Dauer gonad size differences are driven by germline cell number and somatic cell size

In the otherwise wild-type strain expressing *ina-1::mNG* and the germ cell nuclear marker, early dauers had not only longer gonads, but more germ cells than late dauers (Fig. 3A,B), demonstrating that the trend we observe in *daf-2(e1370)* mutants (Fig.2B,D) holds. Gonad length is highly correlated to germ cell number (Fig. 3C). Late dauer germ cells had slightly larger nuclei (Fig. 3D), and all dauer germ cell nuclei had a compacted chromatin appearance (Fig. 3A, inset) characteristic of germ cell quiescence that has been observed in starvation-induced L1 arrest (Belew et al., 2021).

We next asked if germ cell number was the only factor contributing to gonad size differences. After progressive starvation, early wild-type (N2) dauers (Fig. 3E) displayed greater gonad length (~1.7x) (Fig. 3F) and body width (~1.3x) (Fig. 3G) than late dauers. However, the ratio of gonad length to body width also differs, with the early dauer gonads being proportionally larger compared to the body width (~4.5:1) than those of late dauer gonads (~3.5:1) (Fig. 3H), violating an assumption of simple isometric scaling between body and gonad size. This suggests that growth is regulated differently in the gonad vs. the rest of the body.

Unlike the germline, in which cell divisions vary, the somatic gonad cell lineage is invariant (Kimble and Hirsh, 1979; Sulston and Horvitz, 1977) (Fig. 3I). When we examine a somatic gonad nuclear marker (Shaffer and Greenwald, 2022), early and late dauers have the same number of somatic gonad cells (two DTCs, four sheath-spermathecal (SS) cells, and six uterine blast cells Fig. 3J). We further quantified the size of the somatic gonad as the distance between these nuclei. Early dauers have

271 longer individual gonad arms (DTC-SS) than late dauers in addition to an overall greater
272 gonad length (DTC-DTC) (Fig. 3K). The SS-SS measurements represent the length of
273 the bulk of the somatic gonad blast cells found between the two gonad arms that will
274 give rise to the somatic gonad sheath, spermatheca, and uterus; early dauers were also
275 larger than late dauers by this measure (Fig. 3K). Therefore, late dauers have a more
276 compact somatic gonad than early dauers.
277
278 The only somatic gonad cell to be terminally differentiated at this stage of development
279 is the DTC, which is the germline stem cell niche that maintains germ cells in an
280 undifferentiated, stem-like state (Crittenden et al., 2006; Hubbard, 2007; Kimble and
281 White, 1981; Kimble, 2014). Late dauers had smaller DTCs than early dauers, though
282 both had markedly smaller DTC cell size than a continuously-fed L2 control (Fig. 3L,M).
283 Thus, we find two separate mechanisms responsible for the smaller size of the gonad of
284 late dauers, corresponding to their respective cell lineage limitations: while the germline
285 is reduced in cell number, the somatic gonad appears to be more compact with the
286 same number of cells, and the DTCis smaller in cross-section. Because the DTC is
287 required for germ cell proliferation, we next examined the role of this cell in supporting
288 the dauer germline.
289
290 **The dauer germline is maintained in a Notch-independent, quiescent state**
291
292 One necessary factor regulating germline growth is LAG-2 ligand expressed by the DTC
293 activating GLP-1/Notch signaling in the distal germline (Henderson et al., 1994). Under
294 replete conditions, niche signaling via LAG-2 to the GLP-1/Notch receptor in the germ
295 cells is required for their maintenance in a mitotic, undifferentiated state at all
296 developmental stages; both DTC ablation (Kimble and White, 1981) and genetic
297 ablation of Notch signaling (Fox and Schedl, 2015; Kodoyianni et al., 1992) are
298 sufficient to trigger meiosis within hours. However, starvation has been shown to induce
299 a G2-arrested, Notch-independent quiescent state in transiently starved adults (Seidel
300 and Kimble, 2011). We found that primordial germ cells in L1 arrested animals, which
301 are known to be G2-arrested and quiescent (Belew et al., 2021), are also Notch-
302 independent (n=15/15 recovered *glp-1(bn18)* L1 arrested animals were fertile after 24h
303 at 25°C).
304
305 We hypothesized that the germline of both early and late dauers, which are in a *de facto*
306 starved state and known to be G2-arrested (Narbonne and Roy, 2006), is similarly
307 Notch-independent. We investigated this question using worms carrying a temperature
308 sensitive allele of *glp-1*/Notch*, glp-1(bn18),* which at the permissive temperature (16°C)
309 have adequate Notch signaling to remain fertile, but upon shifting to the restrictive
310 temperature (25°C) early in development become sterile due to failure of germline

311 induction or irreversible meiotic entry of germ cells (Fox and Schedl, 2015; Kodoyianni
312 et al., 1992). In adults, signs of meiotic entry appear in distal adult germ cells within 6
313 hrs (Fox and Schedl, 2015; Kodoyianni et al., 1992).
314
315 When continuously-fed populations of *glp-1(bn18)* mutants were shifted to the restrictive
316 temperature for 24 hours (Fig. 4A, and see Methods), nearly all animals singled after
317 the treatment were sterile when shifted back to the permissive temperature (Fig. 4B), as
318 expected. In comparison, when *glp-1(bn18)* dauers–both early and late–were shifted to
319 the restrictive temperature for 24 hours, all recovered as fertile adults at the permissive
320 temperature (Fig. 4B). From this, we conclude that both the early and late dauer
321 germline is in a Notch-independent, quiescent state.
322
323 **Starvation reduces presentation of the stemness cue by the germline stem cell**
324 **niche prior to dauer entry**
325
326 It is not known whether or how LAG-2 protein abundance or localization changes under
327 conditions that induce a Notch-independent, quiescent germline. We used a strain co-
328 expressing an endogenously tagged LAG-2::mNeonGreen (Gordon et al., 2019) and
329 DTC membrane marker (*lag-2p::myrTdTomato,* (Byrd et al., 2014)) to quantify LAG-2
330 abundance in an L2 control compared to both early and late dauers. Both early and late
331 dauers had severely diminished (~10x) LAG-2::mNG signal in the DTC compared to the
332 L2 control but did not significantly differ from one another (Fig. 4C-F). The
333 transcriptional reporter is less active in both dauers compared to the L2, but not by the
334 same magnitude as the LAG-2::mNG (Fig. 4B and 4G). While dauer DTCs produce less
335 *lag-2* gene product than fed L2s, the absolute amount of LAG-2 signaling protein in
336 early vs. late dauer cannot explain the different germline sizes of these groups.
337
338 We next turned to the dynamics with which LAG-2 expression is diminished during the
339 pre-dauer period, the time during which feeding changes germline growth (shown in Fig.
340 2B,C). We combined the LAG-2::mNG endogenous protein tag and the *lag-*
341 *2p::myrTdTomato* transcriptional reporter with the *daf-2(e1370)* allele and performed a
342 timed food removal assay on L2d daf-c animals at 25°C (Fig. 4H, as in Fig. 2). We
343 found that LAG-2::mNG protein abundance is highly responsive to the onset of
344 starvation in L2d. LAG-2::mNG drops from the 20h fed baseline within 5 hours of food
345 removal (Fig 4I-L). Transcription of *lag-2* is known to be lower in late larval animals in
346 unfavorable conditions (low food, high pheromone) that cause reduced DAF-7 signaling
347 (Dalfó et al., 2012; Pekar et al., 2017), and we find that animals in L2d have
348 dramatically less transcription from this reporter than control L2s (Fig. 4M). However,
349 the transcriptional reporter stays fairly steady upon food removal in L2d (Fig. 4M). Thus,
350 reduced *lag-2* transcription cannot be the entire mechanism behind the drop in LAG-

2::mNG abundance upon food removal in L2d; diminished LAG-2::mNG protein stability (at least in comparison to the myristoylated TdTomato reporter) must also play a role.

We conclude that dauer germline is maintained in a Notch-independent state with low levels of the stemness cue LAG-2 expressed by the DTC. The amount of LAG-2 being presented to the germ cells does not differ between early and late dauers, however, suggesting that niche limitations in dauer do not regulate the different gonad sizes between these two cohorts. Instead, the timing at which LAG-2 drops is acutely driven (within 5 hours) by the termination of pre-dauer feeding. We next examined the dynamics of Notch signaling during dauer exit.

Post-dauer Notch-dependence is restored in tandem with a transcription-independent burst of LAG-2 ligand presentation by the germline stem cell niche

We hypothesized that the post-dauer germline would rapidly return to a Notch-dependent state upon germ cell-cycle re-entry during dauer recovery, as proliferating *C. elegans* germ cells are Notch-dependent in other life stages (Austin and Kimble, 1987; Cinquin et al., 2010). We predicted that LAG-2 protein abundance would rapidly increase to meet a post-dauer requirement for Notch signaling. We measured expression in an otherwise wild-type strain of the LAG-2::mNG protein and a *lag-2*-promoter-driven transcriptional reporter upon dauer recovery (see Methods).

At 0 hours of recovery, late dauers had detectable signal of both the LAG-2::mNG protein and the *lag-2* transcriptional reporter (Fig. 5A-D), suggesting that the dauer DTC continues to express the *lag-2* locus and localize LAG-2 protein to the membrane. Dauer expression of *lag-2* reporters in the DTC has been reported previously in *daf-2(e1370)* mutant dauers (Narbonne and Roy, 2006), and here we show that this expression endures through several weeks of dauer. During the first two hours of dauer recovery, LAG-2::mNG protein abundance increases 2-3-fold (Fig. 5A). Surprisingly, we did not observe a corresponding increase in signal from the co-expressed *lag-2p::myrTdTomato* transcriptional reporter (Fig. 5B). Such dynamics suggest that the immediate restoration of LAG-2 on the DTC–much like its initial downregulation upon starvation (Fig. 4I-M)–is post-transcriptionally regulated.

Before drawing this conclusion, we needed to rule out experimental artifacts that could complicate the analysis of the transcriptional reporter. We considered that slow folding of TdTomato fluorescent protein could cause a lag in its transcriptional readout (see Methods), or that post-transcriptional regulation of *lag-2* mRNA could uniquely affect LAG-2 production. We therefore examined the expression of another pair of DTC-expressed markers: a faster-folding, membrane-localized *lag-*

391 *2p::mNeonGreen::PLCδ1^{PH}* (*cpIs122,* (Linden et al., 2017)) and a histone
392 H2B::mTurquoise2 knocked into the endogenous *lag-2* locus with a 2A peptide
393 cleavage site (Medwig-Kinney et al., 2022). This second element will generate a
394 polycistronic mRNA, the translation of which will produce one LAG-2 protein and one
395 H2B::mTurquoise2, meaning that the histone reporter is under the same transcriptional
396 and post-transcriptional, transcript-based regulation (e.g. by 3' UTR-mediated
397 repression by microRNAs or RNA binding proteins, transcript decay, etc.) as the
398 endogenous *lag-2* gene. In the two hours after recovery from dauer, we observe no
399 change in the levels of expression of either the transcriptional membrane (Fig. 5E,G) or
400 polycistronic nuclear reporter (Fig. 5F,H). We conclude that the *lag-2* locus is
401 transcriptionally active in the DTC during dauer–despite the germline being maintained
402 in a Notch-independent state–and LAG-2 is under protein-specific negative regulation
403 that is rapidly alleviated upon dauer exit.
404
405 Given the rapid return of LAG-2 to the DTC surface after dauer exit, we predicted that
406 the germline would become Notch-dependent in the first hours of recovery from dauer.
407 We performed temperature shift experiments during dauer recovery for *glp-1(bn18)*
408 mutant worms (Fig. 5I). Dauer *glp-1(bn18)* mutant animals all recover fertility after an
409 excursion to the restrictive temperature (Fig. 4B). If worms are kept at the restrictive
410 temperature for the first 4 hours of recovery from dauer, the stem-like germ cells remain
411 Notch-independent and the animals recover as fertile adults (Fig. 5J, top, n=39/39).
412 After 6 hours of recovery from dauer at 25°C, ~20% of worms become sterile in
413 adulthood (Fig. 5J, middle, n=7/34). After 8 hours of recovery from dauer at 25°C, more
414 than half of worms will recover as sterile adults (Fig. 5J, bottom, n=25/43). Taken
415 together we see a rebound of LAG-2 protein on the DTC within two hours of recovery
416 from dauer, preceding a return of Notch dependence in the germline between 4-8 hours
417 of recovery. Because dauer exit is asynchronous among individuals (Cassada and
418 Russell, 1975), the precise timing of these events with respect to dauer exit and to one
419 another may be even more tightly coordinated. Other early features of dauer exit–loss of
420 the buccal plug and resumption of pharyngeal pumping–also occur within a two-hour
421 window of removal from dauer conditions (Cassada and Russell, 1975), making the
422 return of LAG-2 on the DTC surface as rapid a response to the end of dauer as any
423 other measured event. This correlation suggests that systemic recovery is more
424 integrated across body systems than pre-dauer changes, which were able to be
425 uncoupled. Our findings establish germline regulation as a central, early feature of
426 dauer recovery.
427
428 **DISCUSSION**
429 Here we report that changes in the germline stem cell niche cue LAG-2 are among the
430 earliest responses both to starvation preceding dauer entry and to environmental cues

431 that allow dauer exit. Reduction of pre-dauer feeding reduces the amount of LAG-2
432 presented by the germline stem cell niche and the proliferation of germline cells.
433 Starved pre-dauer germ cells swiftly become quiescent and complete a single terminal
434 division before dauer entry. The response at the level of germ cell number is dramatic–
435 the most severely starved dauers (wild-type late dauers and *daf-2(e1370)* mutants
436 starved early in L2d) have as few cells in the germline (~5-8) as worms with severe
437 loss-of-function alleles of *glp-1*/Notch receptor gene (Austin and Kimble, 1987), and
438 even fewer germ cells than worms have after early laser ablation of the DTC (Kimble
439 and White, 1981).
440
441 While reduced food intake also slowed the rate of somatic progression towards the
442 L2d/dauer molt, it does not alter somatic cell numbers in the somatic gonad (Fig. 3).
443 Instead, the soma as a whole continues its development through L2d and into dauer
444 while the germline arrests, both in terms of absolute germ cell number and–even more
445 dramatically–rate of germline grown over time (Fig. 2).
446
447 Differences in germline and somatic response to the starvation-induced L1 larval arrest
448 stage have previously been observed, both in differential transcriptional responses
449 (Webster et al., 2022), and chromatin compaction in the germline (Belew et al., 2021;
450 Morao and Ercan, 2021). The L1 arrest state is triggered by complete starvation after
451 hatching (Baugh, 2013; Johnson et al., 1984). Several checkpoints triggered by later
452 starvation arrest somatic development at a later larval stage transition (Schindler et al.,
453 2014), and the somatic gonad relays environmental information to the germline
454 throughout life (Gordon, 2020). We observe that the soma and germline can decouple
455 their development plastically and rapidly in response to changing environmental
456 conditions in the middle of a larval stage.
457
458 Notch signaling via *lag-2* in the nervous system is required both during dauer and for
459 dauer recovery (Ouellet et al., 2008). LAG-2 protein downregulation in the DTC has
460 been observed during worm aging (Aprison et al., 2024 preprint; Singh et al., 2024), and
461 *lag-2* transcription is downregulated via reduced TGF-β signaling after food removal in
462 late larval worms (Dalfó et al., 2012; Pekar et al., 2017). The transition of the germline
463 from a Notch-dependent to a Notch-independent state has been reported during
464 starvation (transient adult starvation (Seidel and Kimble, 2011) and L1 arrest (this
465 paper)), and it should be investigated whether DTC-expressed LAG-2 is also reduced in
466 those contexts. The question remains whether a reduction in LAG-2 signal in response
467 to starvation is the proximal cause of germline quiescence, or whether germline
468 quiescence is a necessary precondition for the germline to tolerate a reduction in LAG-2
469 as a byproduct of starvation.
470

Notably, expression of both endogenously tagged LAG-2 protein and *lag-2* promoter-driven transgenes (Fig. 5 and (Narbonne and Roy, 2006)) remain detectable in dauer–even after an an extended duration of dauer diapause–so the downregulation of *lag-2* during starvation is relative and not absolute. The regulation of LAG-2 in the DTC in our experiments also appears to entail post-translational downregulation upon starvation and during dauer which rapidly ceases at dauer exit.

It has previously been shown that the TGF-β pathway regulates *lag-2* expression in the DTC as part of environmental sensing, including as a response to dauer pheromone and low food, though this work was done in late larvae that had bypassed the dauer decision (Pekar et al., 2017). TGF-β signaling is restored during dauer exit (Ren et al., 1996; Schackwitz et al., 1996), so we predict that *lag-2* transcription eventually rises during recovery from dauer, but apparently not on the rapid time scale of the recovery of LAG-2 protein in the DTC.

While the precise molecular mechanisms linking nutrition to LAG-2 protein expression in the DTC remain to be found, we establish that they proceed even with the field-standard *daf-2(e1370)* class 2 loss-of-function allele of the sole *C. elegans* IIS receptor. Not only is starvation-triggered LAG-2 downregulation DAF-2-independent, but the reproductive consequences of pre-dauer food intake are also the same in *daf-2(e1370)* animals as they are in wild-type worms. Worms that fed before dauer (both early dauers of both genotypes and mutant worms induced to form dauer at high temperature) have normal brood sizes after recovery.

The germline is the only lineage in *C. elegans* with an indeterminate division pattern and variable cell number. It is therefore the only cell population that can respond to starvation by limiting the number of cells it produces. We have demonstrated that this unique flexibility allows germline development to be decoupled from the rest of the dauer entry program earlier than was previously thought. In genetic backgrounds in which animals are able to feed before genetically-induced dauer entry, it has been established that the germline and somatic gonad require AMPK (*lbk-1* and *aak-2*) signaling and DAF-18/PTEN–independent of the DAF-2 IIS receptor–to enter a quiescent state (Narbonne and Roy, 2006; Tenen and Greenwald, 2019). Prior to dauer entry, the temperature-sensitive *glp-1* allele in *daf-2(e1370)* genetic background shifted to the restrictive temperature causes germ cell pachytene arrest during dauer (Narbonne and Roy, 2006). Since these *daf-2(e1370)* mutants feed before entering dauer, this shift to the restrictive temperature occurred during what our work suggests is a Notch-dependent phase of pre-dauer germline growth. We find that after starvation prior to dauer entry, the germline undergoes a reduction in the stemness cue presented

510 by the somatic gonad (also independent of DAF-2) before becoming Notch-independent
511 in dauer.
512
513 Early life stresses are known to affect later life outcomes in a range of organisms and
514 contexts with potential mechanisms ranging from epigenetics to inflammation to
515 hormone signaling to lasting variation in central nervous system development and
516 function (Taylor, 2010). In *C. elegans,* there is precedent for differential reproductive
517 recovery after dauer depending on whether starvation or crowding (high levels of the
518 dauer pheromone) was the primary trigger to dauer entry (Ow et al., 2018). Our
519 progressive starvation protocol involves both starvation and crowding, and future work
520 will probe the contributions of both factors to pre-dauer germline quiescence.
521
522 Taken together, we propose that germline regulation is a key response to both the cues
523 that induce dauer and the withdrawal of those cues in recovery from dauer. Future work
524 will focus on how the germline transitions from a Notch-independent state back to
525 Notch-fueled germline proliferation. One possible driver is nucleotide levels, which have
526 been shown to limit cell division but not cell growth in unicellular organisms (Diehl et al.,
527 2022) and to affect germline growth specifically in non-dauer *C. elegans* (Chi et al.,
528 2016). The rapid restoration of LAG-2 protein to the DTC surface upon withdrawal of
529 dauer-maintenance conditions (Fig. 5) certainly suggests that reestablishing a stem cell
530 niche capable of supporting germline growth is an early and crucial feature of dauer
531 recovery. Our analyses of endogenously tagged LAG-2::mNeonGreen protein recovery
532 vs. transcriptional reporters and a polycistronic reporter altogether suggest that the
533 ligand's increase at the membrane is regulated post-translationally (Fig. 5). Notch
534 signaling is regulated at the protein level in multiple ways (Fortini, 2009; Suarez
535 Rodriguez et al., 2023; Tian et al., 2004; Weinmaster and Fischer, 2011; Wu et al.,
536 2016; Yamamoto et al., 2010), and future work will delve into this aspect of its regulation
537 upon starvation and during dauer exit. Tellingly, in our experiment, LAG-2 increases
538 upon recovery from dauer in the absence of food, suggesting that LAG-2 is actively
539 inhibited by the dauer pheromone rather than actively promoted by nutritional cues.
540
541 Such a mechanism of rapid ligand protein up-regulation by means of alleviated
542 repression could theoretically yield a faster response than upregulation that requires
543 new transcription initiation. However, continuous transcription, translation, and LAG-2
544 protein degradation comes with an energy cost that a dauer worm would only incur if the
545 alternative–slower restoration of LAG-2 protein on the stem cell niche surface–carried
546 an even greater cost of reduced fertility upon return of the germline to Notch-
547 dependence.
548
549

MATERIALS AND METHODS

Sections of this text are adapted from prior Gordon lab publications (Li et al., 2022; Singh et al., 2024), as they describe our standard laboratory practices and equipment.

Strains

We used Wormbase (Sternberg et al., 2024) while conducting this study. Some strains were provided by the CGC, which is funded by NIH Office of Research Infrastructure Programs (P40 OD010440) and are to be requested directly from CGC. The following *C. elegans* strains were obtained from the CGC: N2 (Brenner, 1974), CB1370 *daf-2(e1370)* III (Kimura et al., 1997), CB1372 *daf-7(e1372)* III (Vowels and Thomas, 1992), DG2389 *glp-1(bn18)* III (Kodoyianni et al., 1992).

The following *C. elegans* strains were generously shared by community members or generated previously in our lab:

NK2517 *qIs154(lag-2p:: myr::tdTomato); lag-2(cp193[lag-2:: mNeonGreenˆ3xFlag])* V) (Gordon et al., 2019), KLG034 *cpIs122(lag-2p::mNeonGreen:: PLCδ1^{PH})*II*; lag-2(bmd202* [*lag-2*::P2A::H2B::mTurquoise2^lox511I^2xHA]) V. (Singh et al., 2024), GS9692 *arTi435(rps-27p::2xnls::gfp(flexon)::unc-54 3' UTR* I); *arTi237(ckb-3p::Cre(opti)::tbb-2 3' UTR* X) (Shaffer and Greenwald, 2022).

The following *C. elegans* strains were generated for this paper by crossing alleles from sources that are cited after each strain description: KLG047 *ina-1(qy23[ina-1::mNeonGreen])*;*naSi2*(*mex-5p::H2B::mCherry::nos-2 3'UTR)* II (Jayadev et al., 2019; Linden et al., 2017), KLG050 *daf-2(e1370)* III*; naSi2(mex-5p::H2B::mCherry::nos-2 3'UTR)* II, KLG051 *daf-2(e1370)* III*; qIs154(lag-2p:: myr::tdTomato)* V*; lag-2(cp193[lag-2:: mNeonGreenˆ3xFlag])* V.

Strain maintenance and synchronization

Worm strains were maintained on nematode growth media (NGM) at 16°C unless otherwise specified. Populations were synchronized by bleaching according to a standard egg prep protocol (Stiernagle, 2006).

Dauer formation by progressive starvation and crowding

To more precisely time the formation of facultative dauers, a large, mixed population of well-fed worms was transferred from an uncrowded growth plate to NGM plates seeded with ~70µL of an overnight culture of *E. coli* OP50 bacterial food. Plates were sealed with parafilm and placed at 25°C for the non-temperature-sensitive strains and 16°C for strains containing *daf-2(e1370), daf-7(e1372),* or *glp-1(bn18)* temperature-sensitive alleles. Plates were monitored daily for evidence of starvation (bacterial lawn depleted and worms dispersed). At 25°C this took ~2-4 days and at 16°C this took ~5-7 days

588 The first day starvation was noted became day 0 of starvation. Early dauers were
589 defined as coming from plates that were 5 days or fewer starved, while late dauers were
590 defined as coming from plates that were at least 28 days starved.
591
592 **Brood size assays**
593 All brood size assays were conducted at 16°C to match the necessary conditions of the
594 temperature sensitive strains. After experimental treatment (see below), worms were
595 singly picked to NGM plates seeded with ~70µL *E. coli* OP50. Egg-laying adults were
596 subsequently passaged to a new plate once daily until egg laying stopped. Plates with
597 progeny were kept at 16°C until the oldest worm on the plate had reached L4, after
598 which they were counted. Schematic illustrating this method in Fig. 1E.
599
600 For never-dauer control brood assays, L4 animals of each strain were singled on Day 0.
601 For brood after recovery from constitutive dauer formation, healthy plates of adults were
602 egg prepped; eggs were rolled in M9 overnight at room temperature to obtain a
603 population of arrested L1 larvae. Animals were dropped onto NGM plates seeded with
604 OP50. Plates were sealed with parafilm and put at the restrictive temperature (25°C) to
605 induce dauer formation. Early dauers that were constitutively formed came from plates 5
606 days or fewer after dauer formation; late dauers came from plates at least 28 days after
607 dauer formation. For brood after recovery from progressive starvation, the above
608 protocol was followed to induce dauer. Worms were then isolated by SDS treatment
609 (see next section) and dauers were singly recovered to NGM plates seeded with OP50
610 at 16°C.
611
612 **Dauer isolation protocol**
613 For plates with mixed populations, dauers were isolated with 1% SDS (Karp, 2018) After
614 SDS treatment, the population of recovered animals was placed onto an unseeded
615 NGM plate and the excess liquid was allowed to dry, after which animals were picked to
616 a slide for imaging, were kept on the unseeded plate for the specified number of hours
617 to evaluate short-term recovery, or picked to an NGM plate seeded with OP50 for
618 recovery and brood measurement.
619
620 **Food removal experiments**
621 A synchronized population of *daf-2(e1370); naSi2(mex-5p::H2B::mCherry::nos-2 3'UTR*
622 *II)* L1s was added to NGM plates seeded with OP50 and were put at 25°C to induce
623 constitutive dauer formation. After the specified number of hours (Fig. 2A), animals were
624 rinsed off the seeded plate with M9, recovered to a 15mL conical tube, and were
625 subsequently washed in M9 3-5 times and then rolled in M9 at room temperature for 20
626 minutes before being washed an additional time in M9 to clear bacteria. Washed
627 animals were then transferred to peptone-free plates (recipe from (Eustice et al., 2022))

628 and returned to 25°C to continue to develop. Baseline imaging was done immediately
629 after animals were washed off the food plates. Subsequent imaging done at the
630 specified times (Fig. 2B). For Fig. 2B, animals were subjected to feeding/starvation for
631 the indicated times and then kept at 25°C until the plate visibly had >50% dauers.
632 Animals that appeared to be dauers under a dissecting scope were picked to image for
633 the dauer endpoint of the experiment; only animals with dauer morphology were
634 included in the final dataset. While removal of food in the L1 stage prior to the L1-L2d
635 transition caused L1 developmental arrest, as expected, we found that removal of food
636 after the L2d molt did not inhibit *daf-2(e1370)* animals from progressing through L2d or
637 entering dauer.
638
639 ***glp-1(ts)* temperature shift experiments**
640 Two temperature shift experiments used the temperature-sensitive allele of the Notch
641 receptor *glp-1(bn18)*. To test for *glp-1* dependence during dauer (Fig. 4 A,B), two
642 populations were used. As a control, an unstarved, uncrowded population was reared at
643 16°C, shifted to the restrictive temperature of 25°C for 24 hours, larval worms were
644 singly picked to NGM plates seeded with *E. coli* OP50, and these plates were kept at
645 16°C until adulthood. As two test groups, worms that had been subjected to progressive
646 starvation and crowding at 16°C (both early and late) were shifted to 25°C for 24 hours.
647 After 24 hours, dauers were recovered by SDS isolation and singled to NGM plates
648 seeded with *E. coli* OP50 and kept at 16°C until adulthood. Each plate was
649 subsequently assayed for the presence of progeny.
650
651 To test for when *glp-1* dependence returns after dauer, *glp-1(bn18)* worms were put into
652 dauer by progressive starvation at 16°C, shifted to 25°C overnight, and then SDS
653 isolated, transferred to NGM plates without food and placed back at 25°C for an
654 additional 4, 6, or 8 hours. At that time, the developmentally oldest/largest worms on the
655 plate (the worms that exited dauer first, since dauer exit is asynchronous) were picked
656 as single animals to NGM plates seeded with *E. coli* OP50 food and kept at 16°C until
657 adulthood. After 4 days of recovery at 16°C, each plate was assayed for live larvae, and
658 those that had offspring were scored as fertile. Plates that lacked larvae were imaged at
659 600x magnification in DIC and scored for the presence of embryos in the uterus (fertile)
660 or an absence of gametes (sterile). Embryo retention appeared to be a phenotype of
661 *glp-1(bn18*).
662
663 **Confocal imaging**
664 All images were acquired at room temperature on a Leica DMI8 with an xLIGHT V3
665 confocal spinning disk head (89 North) with a 63× Plan-Apochromat (1.4 NA) objective
666 and an ORCAFusion GenIII sCMOS camera (Hamamatsu Photonics) controlled by
667 microManager. RFPs were excited with a 555 nm laser; GFP and mNG were excited

668 with a 488 nm laser; mTurquoise was excited with a 445 nm laser; DAPI was excited
669 with a 405 nm laser. Z-stacks through the gonad were acquired with a z-step size of 0.3
670 or 0.5 µm as noted. Worms were mounted on agar pads in M9 buffer with 0.01 M
671 sodium azide (VWR (Avantor) Catalog Number 26628-22-8). Some samples were
672 acquired with a 1.6X optical zoom, as indicated in the figure legends. Samples used for
673 fluorescence quantification were acquired with the same laser power, exposure time,
674 and z-step size within the datasets to be compared.
675
676 **Image analysis**
677 Images were processed in FIJI89 (Version: 2.14.1/1.54f).
678
679 **Gonad length and body width measurements**
680 From DIC confocal z-stacks, gonad length was measured from the distal most end of
681 one gonad arm to the distal most end of the other gonad arm using the segmented line
682 tool in FIJI following the general shape of the gonad. Body width was measured from
683 cuticle edge to cuticle edge perpendicular to the gonad using the straight line tool in FIJI
684 across the z-slice that captured the widest part of the body.
685
686 **Somatic gonad marker measurements**
687 *Somatic gonad cell number (Fig. 3J-K):* The strain GS9692 expressing *arTi435(rps-*
688 *27p::2xnls::gfp(flexon)::unc-54 3' UTR)*; *arTi237(ckb-3p::Cre(opti)::tbb-2 3' UTR)*
689 (Shaffer and Greenwald, 2022) was specifically designed to activate enduring GFP
690 expression in the cells of the somatic gonad. We examined this strain in early and late
691 dauers after inducing dauer with progressive starvation and crowding (see above). We
692 always see the expected two DTCs and 10 primordial gonad cells in dauers of any age.
693 Variation in expression levels/tissue depth can sometimes complicate detection of the
694 cell at the center of the gonad primordium (more orange cells in Fig. 3J). Landmarks
695 were selected based on relative position with DTCs at the gonad tips and the next-most-
696 distal fluorescent cells being the SS cells used for measuring.
697
698 *DTC measurement (Fig. 3L-M):* Strain NK2517 *qIs154(lag-2p:: myr::tdTomato); lag-*
699 *2(cp193[lag-2:: mNeonGreenˆ3xFlag]* V*)* was imaged for the DTC membrane marker
700 only at the stages specified in Fig. 3M. A sum projection through ten 0.3 µm z-steps
701 capturing the superficial surface of the DTC was made, traced by hand in FIJI, and the
702 area measured. We chose an L2 control for this experiment because, while the dauer
703 larva is an alternative third larval stage, the worm's reproductive system undergoes
704 morphogenetic changes and changes in cell number during the normal L3 stage. These
705 developmental events are arrested in dauer (Tenen and Greenwald, 2019), making L3 a
706 confounding control for the dauer larvae reproductive system.
707

708 **Dauer recovery experiments**
709 To measure gene expression during recovery, worms were isolated as described above
710 (Dauer isolation protocol), and subsequently split such that some worms were imaged
711 at 0 hours of recovery, and other worms were recovered to NGM plates without food (to
712 isolate withdrawal of dauer maintenance conditions from food-specific cues) for the
713 specified length of time.
714
715 **Reporters of *lag-2* measurement: Endogenously tagged LAG-2::mNG with**
716 **coexpressed membrane TdTomato**
717 Strain NK2517 *qIs154(lag-2p:: myr::tdTomato); lag-2(cp193[lag-2::*
718 *mNeonGreenˆ3xFlag]) V* was used to measure endogenously tagged LAG-2::mNG
719 protein and a coexpressed transcriptional reporter of the *lag-2* promoter. All worms,
720 including controls, were reared at 25°C. TdTomato has a half-time to maturation of one
721 hour at 37°C (Shaner et al., 2004), while mNeonGreen has a half-time to maturation of
722 fewer than ten minutes at 37°C (Shaner et al., 2013) (both will fold slower at worm-
723 rearing temperatures). TdTomato signal is visible in adjacent neurons (Fig. 4 and Fig. 5)
724 and the autofluorescent gut granules of the worm are visible in the channel of the
725 endogenously tagged LAG-2::mNG. These structures were avoided as much as
726 possible during projection, tracing, and measurement of signal.
727
728 Confocal z-stacks were acquired with a 0.3 µm step size. A sum intensity z-projection
729 was created in FIJI consisting of 10 slices representing the superficial half of the cell
730 (from the superficial cell surface to the cross-section of the nucleus). Either one or both
731 DTCs from each worm were analyzed depending on if the gut obscured one. The DTC
732 was hand-traced on the membrane marker RFP channel; that ROI was subsequently
733 used to measure both the RFP (membrane) and GFP (endogenously tagged protein)
734 channels, and slid off the DTC to the adjacent body of the worm to measure the
735 background for both channels. Background subtracted measurements were thus
736 obtained for both Mean Gray Value (mean pixel value in the ROI) and Integrated
737 Density (total pixel value in the region = MGV*area). Integrated density for all samples
738 was normalized to the mean integrated density at the 0h timepoint, so fold-change at 2h
739 time point is shown.
740
741 **Reporters of *lag-2* measurement: Polycistronic histone reporter with coexpressed**
742 **membrane mNeonGreen**
743 We examined another pair of DTC-expressed markers: a faster-folding, membrane-
744 localized *lag-2p::mNeonGreen::PLCδ1^{PH}* (*cpIs122,* (Linden et al., 2017)) and a histone
745 H2B::mTurquoise2 (half-time to maturation of 33.5 minutes, (Goedhart et al., 2012)) that
746 was knocked into the endogenous *lag-2* locus with a 2A peptide cleavage site (Medwig-
747 Kinney et al., 2022). This second element will generate a polycistronic mRNA, the

748 translation of which will produce one LAG-2 protein and one H2B::mTurquoise2,
749 meaning that the histone reporter is under the same transcriptional and post-
750 transcriptional, transcript-based regulation (e.g. by 3' UTR-mediated repression by
751 microRNAs or RNA binding proteins, transcript decay, etc.) as the endogenous *lag-2*
752 gene. The membrane-localized mNeonGreen reporter, on the other hand, will simply
753 come on when the *lag-2* promoter (including the TGF-β-responsive element described
754 by (Pekar et al., 2017)) is active.
755
756 Confocal z-stacks were acquired with a 0.3 µm step size. A sum intensity z-projection
757 through a 6-7 µm depth of the DTC (to capture the entire nucleus in z) was generated in
758 FIJI, the DTC was hand-traced, and membrane fluorescence was measured for the
759 GFP channel in that ROI. Both DTCs from each animal were analyzed in separate
760 projections. A background measurement was made by sliding the DTC ROI onto the
761 adjacent body of the worm. The nuclear histone signal was obtained using an ellipse
762 tool tight around the nucleus in the same z-projection to measure on the CFP channel,
763 and background for the nuclear signal was made by sliding that ROI onto the adjacent
764 body of the worm. Background subtracted measurements were thus obtained for both
765 Mean Gray Value (mean pixel value in the ROI) and Integrated Density (total pixel value
766 in the region, MGV*area). Integrated density for all samples was normalized to the
767 mean integrated density at the 0h timepoint, so fold-change at 2h time point is shown.
768
769 **Statistical analysis**
770 All statistical analysis was done using GraphPad Prism version 10.4.2 for Windows,
771 GraphPad Software, Boston, Massachusetts USA, www.graphpad.com. Specific tests
772 specified in the relevant figure legends.
773 Statistical analysis of fold change shown in 5A, B, E, F; statistical analysis (unpaired t-
774 test) of non-normalized integrated densities for these datasets show the same pattern of
775 significance (that is, only LAG-2::mNG signal changes between 0h and 2h) as the fold
776 change analysis.
777
778 **Author Contributions**
779 Conceptualization: F.A.K. and K.L.G.; Formal analysis: F.A.K.; Investigation: F.A.K. and
780 C.P.M.; Writing – original draft preparation: F.A.K. and K.L.G.; Writing – review and
781 editing: F.A.K., C.P.M., and K.L.G.; Visualization: F.A.K.; Supervision: K.L.G.; Project
782 administration: K.L.G.; Funding acquisition: F.A.K. and K.L.G.
783
784 **Acknowledgements**
785 We thank members of the Gordon Lab and F.A.K. dissertation committee members
786 R.H.D. and D.R.M. for thoughtful comments on the manuscript.
787

Funding
Some strains were provided by the CGC, which is funded by National Institutes of Health Office of Research Infrastructure Programs (P40 OD010440) and are to be requested directly from CGC. Funded by National Institute of General Medical Sciences grant R35GM147704 to K.L.G. and NIGMS Diversity Supplement 3R35GM147704-02S1 to support the work of F.A.K.

Data and resource availability
All relevant data and details of resources can be found within the article.

Conflicts of Interest
The authors declare no conflicts of interest.

FIGURE LEGENDS

Figure 1: Dauer larvae that form after prolonged starvation and crowding have smaller gonads and recover to have smaller broods than dauer larvae that form constitutively.

(A) Gonad length in facultative dauers of control *ina-1::mNG; naSi2(mex-5p::H2B::mCherry::nos-2 3'UTR)* early (n=24) and late (n=28), *daf-2(e1370);naSi2(mex-5p::H2B::mCherry::nos-2 3'UTR)* early (n=19) and late (n=19), *and daf-7(e1372)* early (n=33) and late (n=15). Kruskal-Wallis test statistic=109.2, p<0.0001 with Dunn's correction for multiple comparisons.

(B) Representative differential interference contrast (DIC) microscopy images of facultative mutant early and late dauer gonads. Gonads outlined.

(C) Gonad length in worms reared at 25°C. Control dataset same as in (1A), *daf-2(e1370);naSi2(mex-5p::H2B::mCherry::nos-2 3'UTR)* constitutive early (n=22) and late (n=29) dauers, and *daf-7(e1372)* constitutive early (n=31) and late (n=32) dauers. Kruskal-Wallis test statistic=109.1, p<0.0001 with Dunn's correction for multiple comparisons.

(D) Representative DIC images of constitutive mutant early and late dauer gonads. Gonads outlined.

(E) Schematic for brood size counts in (1F,G).

(F) Brood size of control strain. Never-dauer control (n=15), recovered early (n=21), and recovered late (n=17). Includes animals that died after recovery and animals that were fully sterile, does not include animals that failed to recover from dauer. Kruskal-Wallis test statistic=10.89, p=0.0043 with Dunn's correction for multiple comparisons.

(G) Brood size of *daf-2(e1370);naSi2(mex-5p::H2B::mCherry::nos-2 3'UTR)*. Never-dauer control (n=14), light shaded background indicates constitutive early (n=14) and late (n=12) recovered animals, dark shaded background indicates facultative early

(n=14) and late (n=17) recovered animals. Includes animals that died after recovery and animals that were fully sterile but not animals that failed to recover from dauer. Kruskal-Wallis test statistic=27.76, $p<0.0001$ with Dunn's correction for multiple comparisons. All scale bars 10 μM. Significance indicated as $p<0.0001$ ****; $p<0.005$ **.

Figure 2: Withdrawal of food in the pre-dauer period arrests germ cell proliferation after a single round of division.

(A) Schematic illustrating food removal experiments. Worms moved off food (dashed lines, imaged "Baseline" (2B,C)) and reared until dauer entry (stars, imaged "Dauer" (2B,C). All experiments in Fig. 2 were conducted at 25°C.

(B) Results of experiment detailed in (2A), showing number of germ cell nuclei in *daf-2(e1370);naSi2(mex-5p::H2B::mCherry::nos-2 3'UTR)*. Sample sizes: 12h fed baseline n=31, dauers n=22; 16h fed baseline n=16, dauers n=8; 20h fed baseline n=18, dauers n=13; 24h baseline n=23, dauer=24; continuously fed dauers n=33.

(C) Representative images of *daf-2(e1370);naSi2(mex-5p::H2B::mCherry::nos-2 3'UTR)* (magenta) measured for (2B) at time of food removal (baseline, left) and in dauer (right). Gross structure of the gonad outlined in white.

(D) Experiment as in (2A) with additional +24h endpoint. Darker dots indicate animals in dauer diapause at the time of counting (see 2E). "12h fed" n=13; "12h fed, 24h starved" n=16; "12h fed, 24h fed" n=14, refers to animals that were washed at 12h and returned to food. "12h fed, 72h starved" n=16. Kruskal-Wallis test statistic=39.12; $p<0.0001$ with Dunn's correction for multiple comparisons.

(E) Percentage of worms that had reached the dauer stage under each condition in 2D. In 2D,E, a grey shaded box marks the samples quantified in parallel after 24 hours under experimental conditions, both on and off food.

All scale bars 10 μM. Significance indicated as $p<0.0001$ ****; $p<0.005$ **.

Figure 3: Early and late dauers differ in somatic gonad cell size and germline cell number

(A) Representative images of early and late dauers expressing (green) *ina-1::mNG*, an alpha integrin subunit and (magenta) *naSi2(mex-5p::H2B::mCherry::nos-2 3'UTR*) transgene marking germ cell nuclei. Gonads outlined. Inset image of a germ cell nucleus showing characteristic compacted chromatin morphology of a quiescent germ cell (Belew et al., 2021), scale bar 2 μM.

(B) Germ cell nuclei per animal in *ina-1::mNG;naSi2(mex-5p::H2B::mCherry::nos-2 3'UTR)* early (n=24) and late (n=28) dauers. Mann-Whitney test statistic U=0, $p<0.0001$.

(C) Germ cell number (3B) is highly correlated to the length of the gonad (same samples as in Fig. 1A) for early (light) and late (dark) dauers. $R^2=0.9317$.

868 (D) Nuclear size of early (n=35 nuclei from 3 worms) and late (n=27 nuclei from 4
869 worms) dauers shown in 3A,B. Unpaired t-test statistic t=2.591, df=60; p=0.0120.
870 (E) Representative DIC images of wild type early and late dauer gonads (outlined).
871 (F) Gonad length of wild type early (n=35) and late (n=40) dauers. Mann Whitney test
872 statistic U=18, p<0.0001.
873 (G) Body width of wild type early (n=35) and late (n=40) dauers (same samples as in
874 3F). Mann Whitney test statistic U=17, p<0.0001.
875 (H) Test for isometric scaling of gonad with body. Ratio of gonad length to body width of
876 the same early (n=35) and late (n=40) dauers in 3F,G. Mann-Whitney test statistic
877 U=111, p<0.0001.
878 (I) Illustration of the 12 somatic gonad cells based on (Lints and Hall, 2004), L2/L3
879 molt). We observe the same number of cells in the dauer (K, L). Distal tip cells (DTC),
880 sheath-spermathecal (SS), dorsal uterine (DU), ventral uterine (VU), anchor cell (AC).
881 Germ cells (GC) are separated into two gonad arms. Brackets at top indicate
882 measurements used in (3K).
883 (J) Representative images of early (top) and late (bottom) dauer gonads (outlined) with
884 a somatic gonad-specific nuclear marker *arTi435(rps-27p::2xnls::gfp(flexon)::unc-54 3'*
885 *UTR); arTi237(ckb-3p::Cre(opti)::tbb-2 3' UTR)* (Shaffer and Greenwald, 2022)). Single-
886 slice images colored by fire LUT.
887 (K) Distance between three sets of cells of the somatic gonad in early and late dauers of
888 the strain in (3J). DTC-DTC, DTC-closest SS cell in that same arm, and SS-SS cell
889 across the central region. DTC-DTC, Mann-Whitney test statistic U=31, p<0.0001; DTC-
890 SS, Mann-Whitney test statistic U=193, p<0.0001; SS-SS, Mann-Whitney test statistic
891 U=21, p<0.0001.
892 (L) Area of trace around sum projection of DTC as in (M) in early and late dauers and
893 an L2 control. Welch's ANOVA test statistic=91.91 (2.000, 24.57), p<0.0001 with
894 Dunnett's T3 post-hoc multiple comparisons test.
895 (M) Sum projection through ten 0.3 µm z-slices of the superficial surface of a DTC
896 expressing a membrane-localized transgenic reporter *qIs154(lag-2p:: myr::tdTomato)*
897 for stages described at top.
898 All scale bars (except inset) 10 µM. Significance indicated as p<0.0001 ****; p<0.005 **;
899 p<0.05 *
900
901
902 **Figure 4: Dauer germ cells are arrested in a Notch independent state with a**
903 **reduced DTC presentation of the LAG-2 stemness cue**
904 (A) Schematic illustrating temperature shift experiment testing germline *glp-1*/Notch-
905 independence in dauer. Well-fed control *glp-1(bn18)* mutants were compared dauers of
906 that same genotype from starved and crowded plates. The experiment was repeated for
907 early (<5d in dauer) and late (>4 weeks) dauers.

(B) Worm fertility after (4A). Control (never-dauer population temp shift in parallel with early dauer) n=19, Recovered (early) n=14, Control (temp shift in parallel with late dauer) n=9, Recovered (late) n=15.
(C-E) Sum projection through ten 0.3 µm z-slices of the superficial surface of a DTC expressing endogenously tagged LAG-2 protein (green, *lag-2(cp193[lag-2:: mNeonGreen])*) and a membrane-localized transgenic reporter (magenta, *qIs154(lag-2p:: myr::tdTomato)*) for stages described at top. Each fluorescence channel is shown with identical scaling between treatments, meaning apparent differences in brightness reflect actual differences in signal intensity.
(C-C”) Fed L2 control.
(D-D”) Early dauer.
(E-E”) Late dauer.
(F-G) Integrated density measured for DTCs described in 4C-E. (F) LAG-2::mNG in early (n=15 DTCs) and late (n=13 DTCs) dauers and L2 control (n=14 DTCs). Welch's ANOVA test statistic W=43.65 (2.000, 22.50), p<0.0001 with Dunnett's T3 multiple comparisons.
(G) *lag-2p::myrTdTomato* transcriptional reporter in early (n=15 DTCs) and late (n=13 DTCs) dauers and L2 control (n=14 DTCs). Ordinary one-way ANOVA test statistic F=12.27, p<0.0001 with Tukey's multiple comparisons test.
(H) Schematic of experiment performed for 4I-K. The transgenes shown in 4C-E were crossed into a *daf-2(e1370)* mutant background. Worms were raised on food at 25°C for 20h, imaged, moved off of food, and imaged 5h later.
(I-K) Representative images of worms described in (4H). Sum projection through ten 0.3 µm z-slices of the superficial surface of the DTC coexpressing endogenously tagged LAG-2 protein (green) with DTC membrane-localized transcriptional reporter (magenta).
(I-I”) Fed L2 control animal reared at 25°C.
(J-J”) L2d fed for 20h at 25°C.
(K-K”) Same as in (J) but 5h after food removal at 25°C.
(L-M) Integrated density measured for DTCs described in 4H-K. (L) LAG-2::mNG, 20h L2d fed baseline (n=8) 5h starved (n=12), L2 control (same dataset as shown in (4F)). Welch's ANOVA test statistic W (DFn, DFd)=61.10 (2.000, 17.93), p<0.0001 with Dunnett's T3 multiple comparisons.
(M) Transcriptional reporter *lag-2p:: myr::tdTomato,* 20 h L2d fed baseline (n=8 DTCs) and 5h starved (n=12), L2 control (same dataset as in (4G)). Kruskal-Wallis test statistic=25.41, p<0.0001 with Dunn’s post-hoc correction for multiple comparisons.
All scale bars 10 µM. DTCs outlined in yellow. Significance indicated as p<0.0001 ****; p<0.0005 ***; p<0.005 **.

Figure 5: Removal from dauer maintenance conditions triggers a burst of LAG-2 presentation on the DTC niche that precedes a return to Notch dependence

(A-D) An otherwise wild-type strain coexpressing the endogenously tagged LAG-2 protein *lag-2(cp193[lag-2:: mNeonGreen])* (green in 5C,D) with a membrane-localized transgenic reporter *qIs154(lag-2p:: myr::tdTomato)* (magenta in 5C,D) in dauer (same dataset at "late" in Fig. 4F,G as this was an extension of that experiment and 2 h after removal from dauer maintenance conditions.

(A) Fold change of LAG-2::mNG relative to mean at 0h (0h n=13; 2h n=15). Two high outliers shown at non-proportional distance from the bulk of the data. 2h mean (solid), median (dashed). Mann-Whitney test statistic U=22, p=0.0001.

(B) Fold change of the *lag-2p::myrTdTomato* transcriptional reporter for samples in (5A). Unpaired t-test statistic t=0.6645, df=27; p=0.5120 (ns).

(C-D) Sum projection through ten 0.3 µm z-slices of the superficial surface of a DTC for stages described at top. For 5C,D, each fluorescence channel is shown with identical scaling between time points, meaning apparent differences in brightness reflect actual differences in signal intensity.

(C-C") 0h of recovery.

(D-D") 2h of recovery.

(E-H) Otherwise wild-type strain co-expressing a *lag-2(bmd202* [*lag-2::P2A::H2B::mTurquoise2]*) polycistronic histone reporter knocked into the endogenous *lag-2* locus (magenta in 5G-H) with a *lag-2p::mNeonGreen::PLCδ1^{PH}* membrane-localized transcriptional reporter (green in 5G-H), same treatment at A-D.

(E) Fold change of polycistronic reporter *lag-2(bmd202* [*lag-2*::P2A::H2B::mTurquoise2]) relative to mean at 0h (0h n=46; 2h n=48). Unpaired t-test statistic t=0.5458, df=92, p=0.5865 (ns).

(F) Fold change of *lag-2p::mNeonGreen::PLCδ1^{PH}* transcriptional reporter relative to mean at 0h (0h n=46; 2n=48). Mann-Whitney test statistic U=1031, p=0.5851 (ns).

(G-H) Sum projections through ~20 0.3 µm Z-slices from superficial surface of DTC to deep bottom of nucleus. Acquired with a 1.6x optical zoom.

(G-G") 0h of recovery.

(H-H") 2h of recovery.

(I) Schematic of dauer recovery *glp-1(bn18)* temperature-shift experiment testing the return of Notch-dependence to the germline shown in 5J.

(J) Percentage of animals recovering as fertile vs. sterile results after removal from dauer-maintenance conditions at 25°C for the first 4 h (top, n=39), 6 h (middle, n=34)) and 8 h (bottom, n=43) of recovery.

DTCs outlined in yellow. All scale bars 10 µM.

986 **References**

987 Ailion, M., Thomas, J.H., 2000. Dauer formation induced by high temperatures in
988 Caenorhabditis elegans. Genetics 156, 1047–1067.
989 https://doi.org/10.1093/genetics/156.3.1047.
990 Angelo, G., Van Gilst, M.R., 2009. Starvation protects germline stem cells and extends
991 reproductive longevity in C. elegans. Science 326, 954–958.
992 https://doi.org/10.1126/science.1178343.
993 Aprison, E.Z., Dzitoyeva, S., Ruvinsky, I., 2024. The roles of TGFβ and serotonin signaling in
994 regulating proliferation of oocyte precursors and germline aging. bioRxiv.
995 Austin, J., Kimble, J., 1987. glp-1 is required in the germ line for regulation of the decision
996 between mitosis and meiosis in C. elegans. Cell 51, 589–599. https://doi.org/10.1016/0092-
997 8674(87)90128-0.
998 Barbieri, M., Bonafè, M., Franceschi, C., Paolisso, G., 2003. Insulin/IGF-I-signaling pathway: an
999 evolutionarily conserved mechanism of longevity from yeast to humans. Am. J. Physiol.
1000 Endocrinol. Metab. 285, E1064-71. https://doi.org/10.1152/ajpendo.00296.2003.
1001 Baugh, L.R., 2013. To grow or not to grow: nutritional control of development during
1002 Caenorhabditis elegans L1 arrest. Genetics 194, 539–555.
1003 https://doi.org/10.1534/genetics.113.150847.
1004 Belew, M.D., Chien, E., Wong, M., Michael, W.M., 2021. A global chromatin compaction
1005 pathway that represses germline gene expression during starvation. J. Cell Biol. 220.
1006 https://doi.org/10.1083/jcb.202009197.
1007 Blackwell, T.K., Steinbaugh, M.J., Hourihan, J.M., Ewald, C.Y., Isik, M., 2015. SKN-1/Nrf, stress
1008 responses, and aging in Caenorhabditis elegans. Free Radic. Biol. Med. 88, 290–301.
1009 https://doi.org/10.1016/j.freeradbiomed.2015.06.008.
1010 Brenner, S., 1974. THE GENETICS OF *caenorhabditis elegans*. Genetics 77, 71–94.
1011 https://doi.org/10.1093/genetics/77.1.71.
1012 Byrd, D.T., Knobel, K., Affeldt, K., Crittenden, S.L., Kimble, J., 2014. A DTC niche plexus
1013 surrounds the germline stem cell pool in Caenorhabditis elegans. PLoS ONE 9, e88372.
1014 https://doi.org/10.1371/journal.pone.0088372.
1015 Cassada, R.C., Russell, R.L., 1975. The dauerlarva, a post-embryonic developmental variant of
1016 the nematode Caenorhabditis elegans. Dev. Biol. 46, 326–342.
1017 https://doi.org/10.1016/0012-1606(75)90109-8.
1018 Chi, C., Ronai, D., Than, M.T., Walker, C.J., Sewell, A.K., Han, M., 2016. Nucleotide levels
1019 regulate germline proliferation through modulating GLP-1/Notch signaling in C. elegans.
1020 Genes Dev. 30, 307–320. https://doi.org/10.1101/gad.275107.115.
1021 Cinquin, O., Crittenden, S.L., Morgan, D.E., Kimble, J., 2010. Progression from a stem cell-like
1022 state to early differentiation in the C. elegans germ line. Proc Natl Acad Sci USA 107,
1023 2048–2053. https://doi.org/10.1073/pnas.0912704107.
1024 Claeys, I., Simonet, G., Poels, J., Van Loy, T., Vercammen, L., De Loof, A., Vanden Broeck, J.,
1025 2002. Insulin-related peptides and their conserved signal transduction pathway. Peptides
1026 23, 807–816. https://doi.org/10.1016/s0196-9781(01)00666-0.
1027 Corsi, A.K., Wightman, B., Chalfie, M., 2015. A Transparent Window into Biology: A Primer on
1028 Caenorhabditis elegans. Genetics 200, 387–407.
1029 https://doi.org/10.1534/genetics.115.176099.

1030 Crittenden, S.L., Leonhard, K.A., Byrd, D.T., Kimble, J., 2006. Cellular analyses of the mitotic
1031 region in the Caenorhabditis elegans adult germ line. Mol. Biol. Cell 17, 3051–3061.
1032 https://doi.org/10.1091/mbc.E06-03-0170.
1033 Dalfó, D., Michaelson, D., Hubbard, E.J.A., 2012. Sensory regulation of the C. elegans germline
1034 through TGF-β-dependent signaling in the niche. Curr. Biol. 22, 712–719.
1035 https://doi.org/10.1016/j.cub.2012.02.064.
1036 Das, D., Arur, S., 2017. Conserved insulin signaling in the regulation of oocyte growth,
1037 development, and maturation. Mol. Reprod. Dev. 84, 444–459.
1038 https://doi.org/10.1002/mrd.22806.
1039 Diehl, F.F., Miettinen, T.P., Elbashir, R., Nabel, C.S., Darnell, A.M., Do, B.T., Manalis, S.R.,
1040 Lewis, C.A., Vander Heiden, M.G., 2022. Nucleotide imbalance decouples cell growth from
1041 cell proliferation. Nat. Cell Biol. 24, 1252–1264. https://doi.org/10.1038/s41556-022-00965-
1042 1.
1043 Erkut, C., Kurzchalia, T.V., 2015. The C. elegans dauer larva as a paradigm to study metabolic
1044 suppression and desiccation tolerance. Planta 242, 389–396.
1045 https://doi.org/10.1007/s00425-015-2300-x.
1046 Eustice, M., Konzman, D., Reece, J.M., Ghosh, S., Alston, J., Hansen, T., Golden, A., Bond,
1047 M.R., Abramowitz, L.K., Hanover, J.A., 2022. Nutrient sensing pathways regulating adult
1048 reproductive diapause in C. elegans. PLoS ONE 17, e0274076.
1049 https://doi.org/10.1371/journal.pone.0274076.
1050 Fortini, M.E., 2009. Notch signaling: the core pathway and its posttranslational regulation. Dev.
1051 Cell 16, 633–647. https://doi.org/10.1016/j.devcel.2009.03.010.
1052 Fox, P.M., Schedl, T., 2015. Analysis of Germline Stem Cell Differentiation Following Loss of
1053 GLP-1 Notch Activity in Caenorhabditis elegans. Genetics 201, 167–184.
1054 https://doi.org/10.1534/genetics.115.178061.
1055 Gems, D., Sutton, A.J., Sundermeyer, M.L., Albert, P.S., King, K.V., Edgley, M.L., Larsen, P.L.,
1056 Riddle, D.L., 1998. Two pleiotropic classes of daf-2 mutation affect larval arrest, adult
1057 behavior, reproduction and longevity in Caenorhabditis elegans. Genetics 150, 129–155.
1058 https://doi.org/10.1093/genetics/150.1.129.
1059 Goedhart, J., von Stetten, D., Noirclerc-Savoye, M., Lelimousin, M., Joosen, L., Hink, M.A., van
1060 Weeren, L., Gadella, T.W.J., Royant, A., 2012. Structure-guided evolution of cyan
1061 fluorescent proteins towards a quantum yield of 93%. Nat. Commun. 3, 751.
1062 https://doi.org/10.1038/ncomms1738.
1063 Golden, J.W., Riddle, D.L., 1984a. The Caenorhabditis elegans dauer larva: developmental
1064 effects of pheromone, food, and temperature. Dev. Biol. 102, 368–378.
1065 https://doi.org/10.1016/0012-1606(84)90201-X.
1066 Golden, J.W., Riddle, D.L., 1984b. A pheromone-induced developmental switch in
1067 Caenorhabditis elegans: Temperature-sensitive mutants reveal a wild-type temperature-
1068 dependent process. Proc Natl Acad Sci USA 81, 819–823.
1069 https://doi.org/10.1073/pnas.81.3.819.
1070 Gordon, K.L., Payne, S.G., Linden-High, L.M., Pani, A.M., Goldstein, B., Hubbard, E.J.A.,
1071 Sherwood, D.R., 2019. Ectopic Germ Cells Can Induce Niche-like Enwrapment by
1072 Neighboring Body Wall Muscle. Curr. Biol. 29, 823-833.e5.
1073 https://doi.org/10.1016/j.cub.2019.01.056.

1074 Gordon, K., 2020. Recent Advances in the Genetic, Anatomical, and Environmental Regulation
1075 of the C. elegans Germ Line Progenitor Zone. J. Dev. Biol. 8.
1076 https://doi.org/10.3390/jdb8030014.
1077 Greer, E.R., Pérez, C.L., Van Gilst, M.R., Lee, B.H., Ashrafi, K., 2008. Neural and molecular
1078 dissection of a C. elegans sensory circuit that regulates fat and feeding. Cell Metab. 8,
1079 118–131. https://doi.org/10.1016/j.cmet.2008.06.005.
1080 Hand, S.C., Denlinger, D.L., Podrabsky, J.E., Roy, R., 2016. Mechanisms of animal diapause:
1081 recent developments from nematodes, crustaceans, insects, and fish. Am. J. Physiol.
1082 Regul. Integr. Comp. Physiol. 310, R1193-211. https://doi.org/10.1152/ajpregu.00250.2015.
1083 Harsimran Kaur Gill, Gaurav Goyal, Gurminder Chahil, 2017. Insect diapause: A review. JAST-
1084 A 7. https://doi.org/10.17265/2161-6256/2017.07.002.
1085 Henderson, S.T., Gao, D., Lambie, E.J., Kimble, J., 1994. lag-2 may encode a signaling ligand
1086 for the GLP-1 and LIN-12 receptors of C. elegans. Development 120, 2913–2924.
1087 https://doi.org/10.1242/dev.120.10.2913.
1088 Hubbard, E.J.A., 2007. Caenorhabditis elegans germ line: a model for stem cell biology. Dev.
1089 Dyn. 236, 3343–3357. https://doi.org/10.1002/dvdy.21335.
1090 Jayadev, R., Chi, Q., Keeley, D.P., Hastie, E.L., Kelley, L.C., Sherwood, D.R., 2019. α-Integrins
1091 dictate distinct modes of type IV collagen recruitment to basement membranes. J. Cell Biol.
1092 218, 3098–3116. https://doi.org/10.1083/jcb.201903124.
1093 Johnson, T.E., Mitchell, D.H., Kline, S., Kemal, R., Foy, J., 1984. Arresting development arrests
1094 aging in the nematode Caenorhabditis elegans. Mech. Ageing Dev. 28, 23–40.
1095 https://doi.org/10.1016/0047-6374(84)90150-7.
1096 Karp, X., 2018. Working with dauer larvae. WormBook 2018, 1–19.
1097 https://doi.org/10.1895/wormbook.1.180.1.
1098 Kenyon, C., Chang, J., Gensch, E., Rudner, A., Tabtiang, R., 1993. A C. elegans mutant that
1099 lives twice as long as wild type. Nature 366, 461–464. https://doi.org/10.1038/366461a0.
1100 Kimble, J., Crittenden, S.L., 2005. Germline proliferation and its control. WormBook 1–14.
1101 https://doi.org/10.1895/wormbook.1.13.1.
1102 Kimble, J., Hirsh, D., 1979. The postembryonic cell lineages of the hermaphrodite and male
1103 gonads in Caenorhabditis elegans. Dev. Biol. 70, 396–417. https://doi.org/10.1016/0012-
1104 1606(79)90035-6.
1105 Kimble, J.E., White, J.G., 1981. On the control of germ cell development in Caenorhabditis
1106 elegans. Dev. Biol. 81, 208–219. https://doi.org/10.1016/0012-1606(81)90284-0.
1107 Kimble, J., 2014. C. elegans germline stem cells and their niche. StemBook.
1108 https://doi.org/10.3824/stembook.1.95.1.
1109 Kimura, K.D., Tissenbaum, H.A., Liu, Y., Ruvkun, G., 1997. daf-2, an insulin receptor-like gene
1110 that regulates longevity and diapause in Caenorhabditis elegans. Science 277, 942–946.
1111 https://doi.org/10.1126/science.277.5328.942.
1112 Kim, S., Paik, Y.-K., 2008. Developmental and reproductive consequences of prolonged non-
1113 aging dauer in Caenorhabditis elegans. Biochem. Biophys. Res. Commun. 368, 588–592.
1114 https://doi.org/10.1016/j.bbrc.2008.01.131.
1115 Klass, M., Hirsh, D., 1976. Non-ageing developmental variant of Caenorhabditis elegans.
1116 Nature 260, 523–525. https://doi.org/10.1038/260523a0.
1117 Kodoyianni, V., Maine, E.M., Kimble, J., 1992. Molecular basis of loss-of-function mutations in

1118 the glp-1 gene of Caenorhabditis elegans. Mol. Biol. Cell 3, 1199–1213.
1119 https://doi.org/10.1091/mbc.3.11.1199.
1120 Linden, L.M., Gordon, K.L., Pani, A.M., Payne, S.G., Garde, A., Burkholder, D., Chi, Q.,
1121 Goldstein, B., Sherwood, D.R., 2017. Identification of regulators of germ stem cell
1122 enwrapment by its niche in C. elegans. Dev. Biol. 429, 271–284.
1123 https://doi.org/10.1016/j.ydbio.2017.06.019.
1124 Lints, R., Hall, D.H., 2004. WormAtlas Hermaphrodite Handbook - Reproductive System -
1125 Somatic Gonad. WormAtlas. https://doi.org/10.3908/wormatlas.1.22.
1126 Li, X., Singh, N., Miller, C., Washington, I., Sosseh, B., Gordon, K.L., 2022. The C. elegans
1127 gonadal sheath Sh1 cells extend asymmetrically over a differentiating germ cell population
1128 in the proliferative zone. eLife 11. https://doi.org/10.7554/eLife.75497.
1129 McGehee, A., 2019. The GLR-1 phenotypes of the daf-7(e1372) allele are not temperature
1130 sensitive. MicroPubl. Biol. 2019. https://doi.org/10.17912/micropub.biology.000158.
1131 Medwig-Kinney, T.N., Sirota, S.S., Gibney, T.V., Pani, A.M., Matus, D.Q., 2022. An in vivo
1132 toolkit to visualize endogenous LAG-2/Delta and LIN-12/Notch signaling in C. elegans.
1133 MicroPubl. Biol. 2022. https://doi.org/10.17912/micropub.biology.000602.
1134 Morao, A.K., Ercan, S., 2021. Hatched and starved: Two chromatin compaction mechanisms
1135 join forces to silence germ cell genome. J. Cell Biol. 220.
1136 https://doi.org/10.1083/jcb.202107026.
1137 Murphy, C.T., Hu, P.J., 2013. Insulin/insulin-like growth factor signaling in C. elegans.
1138 WormBook 1–43. https://doi.org/10.1895/wormbook.1.164.1.
1139 Narbonne, P., Roy, R., 2006. Inhibition of germline proliferation during C. elegans dauer
1140 development requires PTEN, LKB1 and AMPK signalling. Development 133, 611–619.
1141 https://doi.org/10.1242/dev.02232.
1142 Ouellet, J., Li, S., Roy, R., 2008. Notch signalling is required for both dauer maintenance and
1143 recovery in C. elegans. Development 135, 2583–2592. https://doi.org/10.1242/dev.012435.
1144 Ow, M.C., Borziak, K., Nichitean, A.M., Dorus, S., Hall, S.E., 2018. Early experiences mediate
1145 distinct adult gene expression and reproductive programs in Caenorhabditis elegans. PLoS
1146 Genet. 14, e1007219. https://doi.org/10.1371/journal.pgen.1007219.
1147 Pekar, O., Ow, M.C., Hui, K.Y., Noyes, M.B., Hall, S.E., Hubbard, E.J.A., 2017. Linking the
1148 environment, DAF-7/TGFβ signaling and LAG-2/DSL ligand expression in the germline
1149 stem cell niche. Development 144, 2896–2906. https://doi.org/10.1242/dev.147660.
1150 Renfree, M.B., Fenelon, J.C., 2017. The enigma of embryonic diapause. Development 144,
1151 3199–3210. https://doi.org/10.1242/dev.148213.
1152 Ren, P., Lim, C.S., Johnsen, R., Albert, P.S., Pilgrim, D., Riddle, D.L., 1996. Control of C.
1153 elegans larval development by neuronal expression of a TGF-beta homolog. Science 274,
1154 1389–1391. https://doi.org/10.1126/science.274.5291.1389.
1155 Schackwitz, W.S., Inoue, T., Thomas, J.H., 1996. Chemosensory neurons function in parallel to
1156 mediate a pheromone response in C. elegans. Neuron 17, 719–728.
1157 https://doi.org/10.1016/s0896-6273(00)80203-2.
1158 Schindler, A.J., Baugh, L.R., Sherwood, D.R., 2014. Identification of late larval stage
1159 developmental checkpoints in Caenorhabditis elegans regulated by insulin/IGF and steroid
1160 hormone signaling pathways. PLoS Genet. 10, e1004426.
1161 https://doi.org/10.1371/journal.pgen.1004426.

1162 Schluter, D., Price, T.D., Rowe, L., 1991. Conflicting selection pressures and life history trade-
1163 offs. Proc. R. Soc. Lond. B 246, 11–17. https://doi.org/10.1098/rspb.1991.0118.
1164 Seidel, H.S., Kimble, J., 2011. The oogenic germline starvation response in C. elegans. PLoS
1165 ONE 6, e28074. https://doi.org/10.1371/journal.pone.0028074.
1166 Shaffer, J.M., Greenwald, I., 2022. Floxed exon (Flexon): A flexibly positioned stop cassette for
1167 recombinase-mediated conditional gene expression. Proc Natl Acad Sci USA 119.
1168 https://doi.org/10.1073/pnas.2117451119.
1169 Shaner, N.C., Campbell, R.E., Steinbach, P.A., Giepmans, B.N.G., Palmer, A.E., Tsien, R.Y.,
1170 2004. Improved monomeric red, orange and yellow fluorescent proteins derived from
1171 Discosoma sp. red fluorescent protein. Nat. Biotechnol. 22, 1567–1572.
1172 https://doi.org/10.1038/nbt1037.
1173 Shaner, N.C., Lambert, G.G., Chammas, A., Ni, Y., Cranfill, P.J., Baird, M.A., Sell, B.R., Allen,
1174 J.R., Day, R.N., Israelsson, M., Davidson, M.W., Wang, J., 2013. A bright monomeric green
1175 fluorescent protein derived from Branchiostoma lanceolatum. Nat. Methods 10, 407–409.
1176 https://doi.org/10.1038/nmeth.2413.
1177 Singh, N., Zhang, P., Li, K.J., Gordon, K.L., 2024. The Rac pathway prevents cell fragmentation
1178 in a nonprotrusively migrating leader cell during C. elegans gonad organogenesis. Curr.
1179 Biol. 34, 2387-2402.e5. https://doi.org/10.1016/j.cub.2024.04.073.
1180 Sternberg, P.W., Van Auken, K., Wang, Q., Wright, A., Yook, K., Zarowiecki, M., Arnaboldi, V.,
1181 Becerra, A., Brown, S., Cain, S., Chan, J., Chen, W.J., Cho, J., Davis, P., Diamantakis, S.,
1182 Dyer, S., Grigoriadis, D., Grove, C.A., Harris, T., Howe, K., Stein, L., 2024. WormBase
1183 2024: status and transitioning to Alliance infrastructure. Genetics 227.
1184 https://doi.org/10.1093/genetics/iyae050.
1185 Stiernagle, T., 2006. Maintenance of C. elegans. WormBook 1–11.
1186 https://doi.org/10.1895/wormbook.1.101.1.
1187 Suarez Rodriguez, F., Sanlidag, S., Sahlgren, C., 2023. Mechanical regulation of the Notch
1188 signaling pathway. Curr. Opin. Cell Biol. 85, 102244.
1189 https://doi.org/10.1016/j.ceb.2023.102244.
1190 Sulston, J.E., Horvitz, H.R., 1977. Post-embryonic cell lineages of the nematode,
1191 Caenorhabditis elegans. Dev. Biol. 56, 110–156. https://doi.org/10.1016/0012-
1192 1606(77)90158-0.
1193 Sulston, J.E., Schierenberg, E., White, J.G., Thomson, J.N., 1983. The embryonic cell lineage of
1194 the nematode Caenorhabditis elegans. Dev. Biol. 100, 64–119.
1195 https://doi.org/10.1016/0012-1606(83)90201-4.
1196 Taylor, S.E., 2010. Mechanisms linking early life stress to adult health outcomes. Proc Natl
1197 Acad Sci USA 107, 8507–8512. https://doi.org/10.1073/pnas.1003890107.
1198 Tenen, C.C., Greenwald, I., 2019. Cell Non-autonomous Function of daf-18/PTEN in the
1199 Somatic Gonad Coordinates Somatic Gonad and Germline Development in C. elegans
1200 Dauer Larvae. Curr. Biol. 29, 1064-1072.e8. https://doi.org/10.1016/j.cub.2019.01.076.
1201 Tian, X., Hansen, D., Schedl, T., Skeath, J.B., 2004. Epsin potentiates Notch pathway activity in
1202 Drosophila and C. elegans. Development 131, 5807–5815.
1203 https://doi.org/10.1242/dev.01459.
1204 Trent, C., Tsuing, N., Horvitz, H.R., 1983. Egg-laying defective mutants of the nematode
1205 Caenorhabditis elegans. Genetics 104, 619–647.

1206 https://doi.org/10.1093/genetics/104.4.619.
1207 Tullet, J.M.A., Hertweck, M., An, J.H., Baker, J., Hwang, J.Y., Liu, S., Oliveira, R.P., Baumeister,
1208 R., Blackwell, T.K., 2008. Direct inhibition of the longevity-promoting factor SKN-1 by
1209 insulin-like signaling in C. elegans. Cell 132, 1025–1038.
1210 https://doi.org/10.1016/j.cell.2008.01.030.
1211 Vowels, J.J., Thomas, J.H., 1992. Genetic analysis of chemosensory control of dauer formation
1212 in Caenorhabditis elegans. Genetics 130, 105–123.
1213 https://doi.org/10.1093/genetics/130.1.105.
1214 Wadsworth, W.G., Riddle, D.L., 1989. Developmental regulation of energy metabolism in
1215 Caenorhabditis elegans. Dev. Biol. 132, 167–173. https://doi.org/10.1016/0012-
1216 1606(89)90214-5.
1217 Webster, A.K., Chitrakar, R., Taylor, S.M., Baugh, L.R., 2022. Alternative somatic and germline
1218 gene-regulatory strategies during starvation-induced developmental arrest. Cell Rep. 41,
1219 111473. https://doi.org/10.1016/j.celrep.2022.111473.
1220 Webster, A.K., Jordan, J.M., Hibshman, J.D., Chitrakar, R., Baugh, L.R., 2018.
1221 Transgenerational Effects of Extended Dauer Diapause on Starvation Survival and Gene
1222 Expression Plasticity in Caenorhabditis elegans. Genetics 210, 263–274.
1223 https://doi.org/10.1534/genetics.118.301250.
1224 Weinmaster, G., Fischer, J.A., 2011. Notch ligand ubiquitylation: what is it good for? Dev. Cell
1225 21, 134–144. https://doi.org/10.1016/j.devcel.2011.06.006.
1226 Wilsterman, K., Ballinger, M.A., Williams, C.M., 2021. A unifying, eco-physiological framework
1227 for animal dormancy. Funct. Ecol. 35, 11–31. https://doi.org/10.1111/1365-2435.13718.
1228 Wu, X., Fleming, A., Ricketts, T., Pavel, M., Virgin, H., Menzies, F.M., Rubinsztein, D.C., 2016.
1229 Autophagy regulates Notch degradation and modulates stem cell development and
1230 neurogenesis. Nat. Commun. 7, 10533. https://doi.org/10.1038/ncomms10533.
1231 Yamamoto, S., Charng, W.-L., Bellen, H.J., 2010. Endocytosis and intracellular trafficking of
1232 Notch and its ligands. Curr. Top. Dev. Biol. 92, 165–200. https://doi.org/10.1016/S0070-
1233 2153(10)92005-X.

Figure 1:

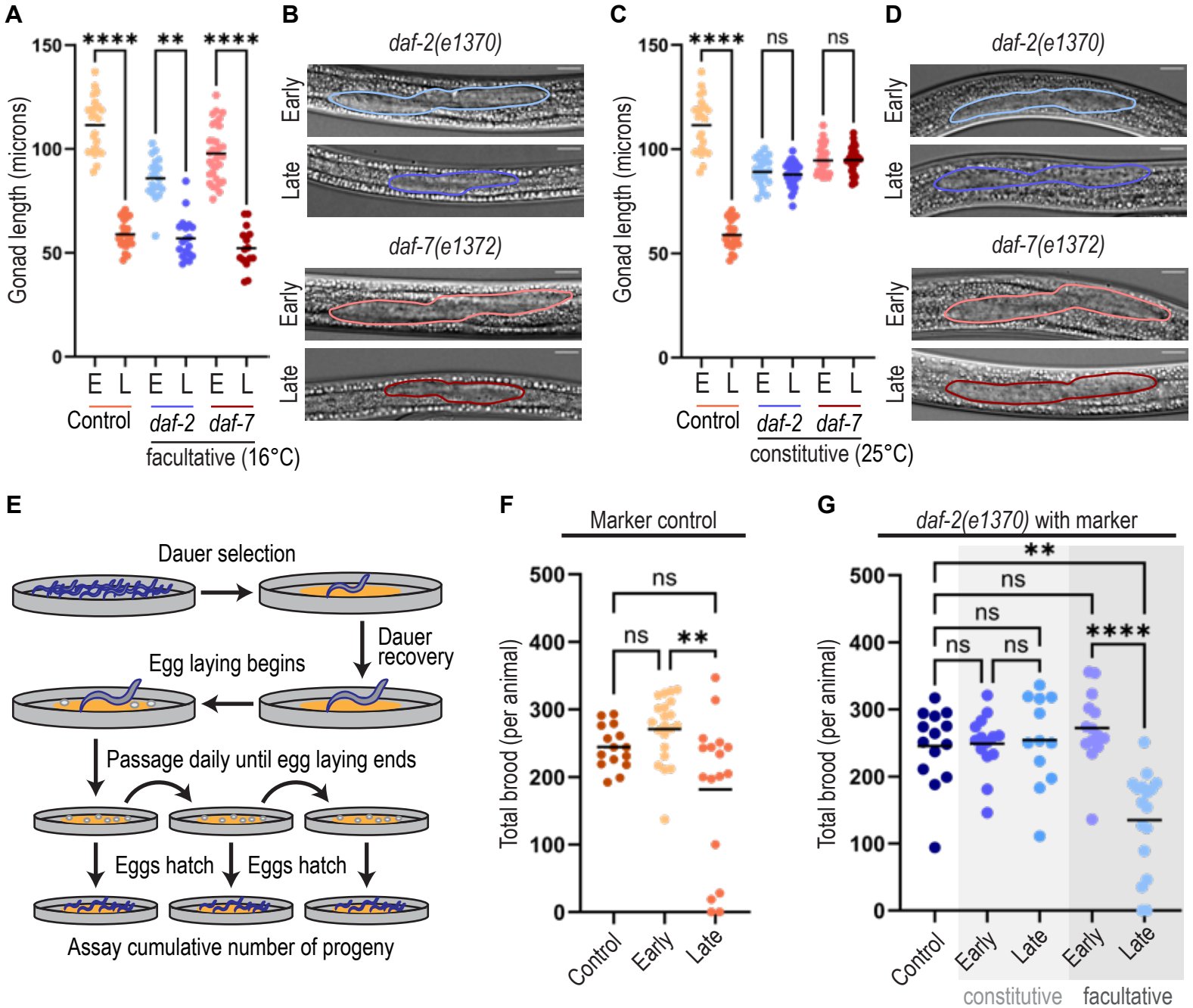
A
B
C
D
E
F
G
Gonad length (microns)
150
100
50
0
****
**
ns
E L E L E L
Control
daf-2
daf-7
facultative (16°C)
constitutive (25°C)
daf-2(e1370)
daf-7(e1372)
Early
Late
Dauer selection
Dauer recovery
Egg laying begins
Passage daily until egg laying ends
Eggs hatch
Assay cumulative number of progeny
Marker control
daf-2(e1370) with marker
Total brood (per animal)
500
400
300
200
100
0
Control
constitutive
facultative

Figure 2:

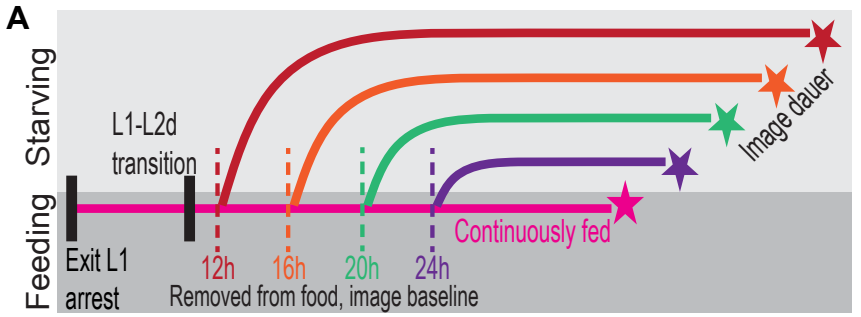
A
Starving
Feeding
L1-L2d
transition
Exit L1
arrest
12h
16h
20h
24h
Removed from food, image baseline
Image dauer
Continuously fed

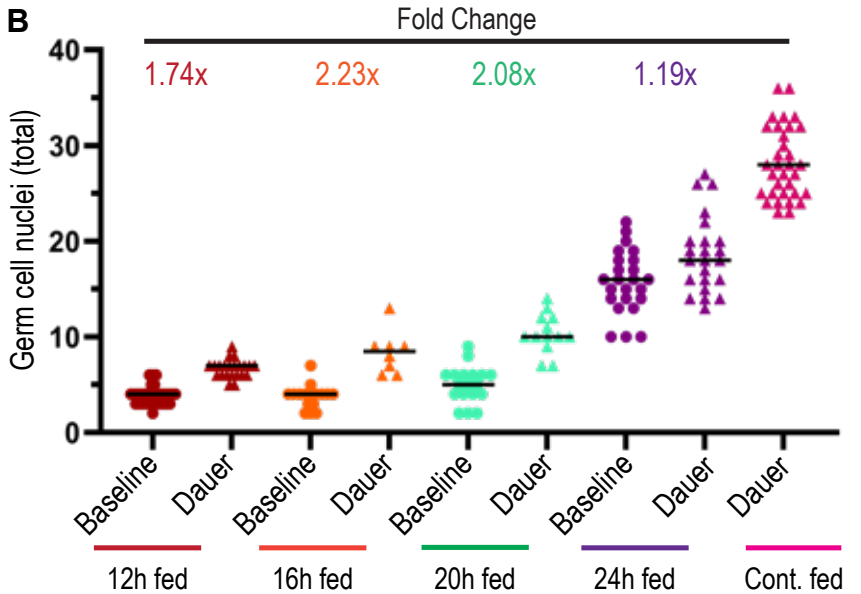
B
Fold Change
1.74x
2.23x
2.08x
1.19x
Germ cell nuclei (total)
40
30
20
10
0
Baseline
Dauer
Baseline
Dauer
Baseline
Dauer
Baseline
Dauer
Dauer
12h fed
16h fed
20h fed
24h fed
Cont. fed

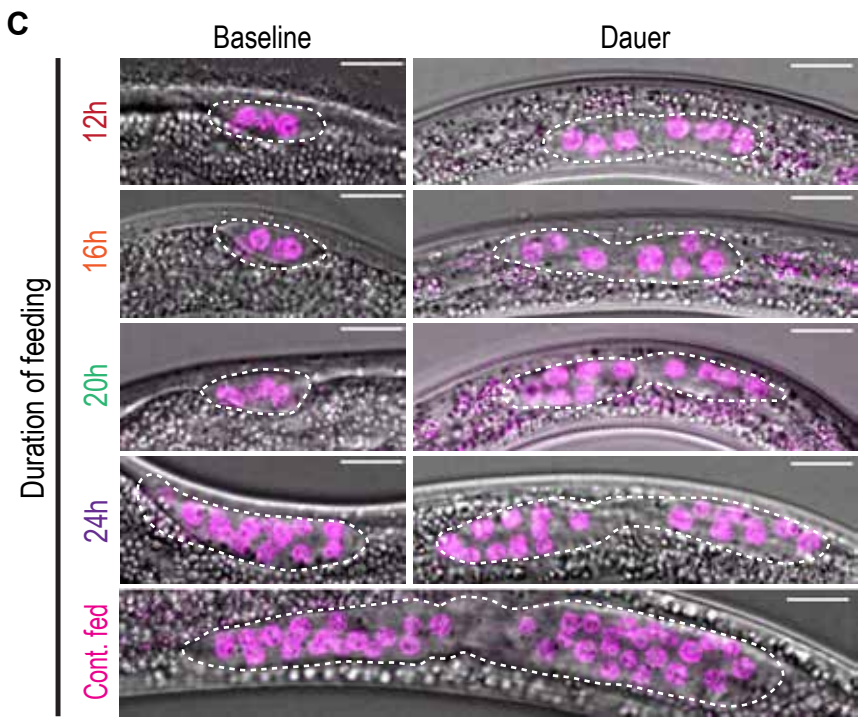
C
Baseline
Dauer
Duration of feeding
12h
16h
20h
24h
Cont. fed

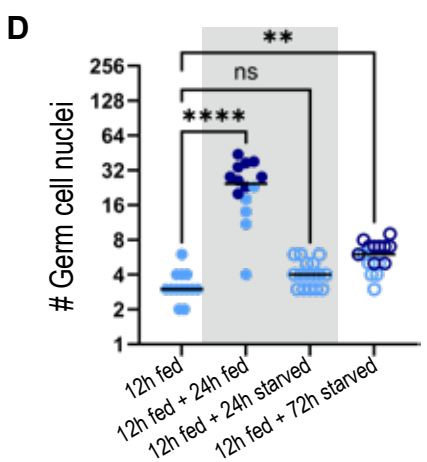
D
Germ cell nuclei
256
128
64
32
16
8
4
2
1
**
ns
****
12h fed
12h fed + 24h fed
12h fed + 24h starved
12h fed + 72h starved

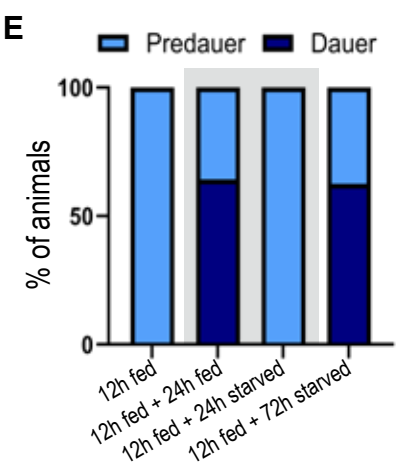
E
Predauer
Dauer
% of animals
100
50
0
12h fed
12h fed + 24h fed
12h fed + 24h starved
12h fed + 72h starved

Figure 3:

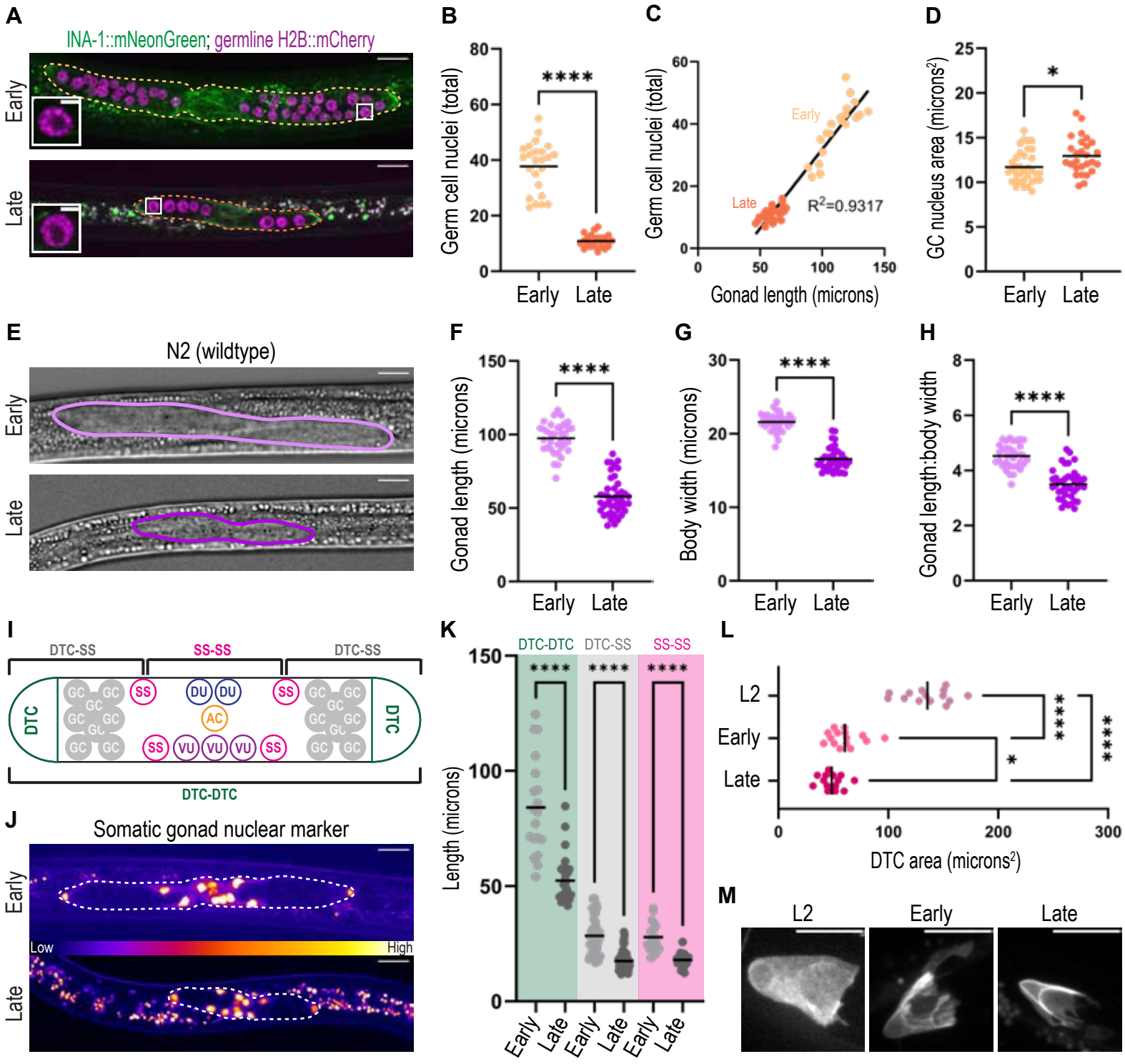
A
INA-1::mNeonGreen; germline H2B::mCherry
Early
Late
B
Germ cell nuclei (total)
****
Early
Late
C
Germ cell nuclei (total)
Early
Late
R²=0.9317
Gonad length (microns)
D
GC nucleus area (microns²)
*
Early
Late
E
N2 (wildtype)
Early
Late
F
Gonad length (microns)
****
Early
Late
G
Body width (microns)
****
Early
Late
H
Gonad length:body width
****
Early
Late
I
DTC-SS
SS-SS
DTC-SS
DTC
SS
DU
AC
VU
GC
DTC
DTC-DTC
J
Somatic gonad nuclear marker
Early
Low
High
Late
K
DTC-DTC
DTC-SS
SS-SS
Length (microns)
****
Early
Late
L
L2
Early
Late
DTC area (microns²)
*
****
M
L2
Early
Late

Figure 4:

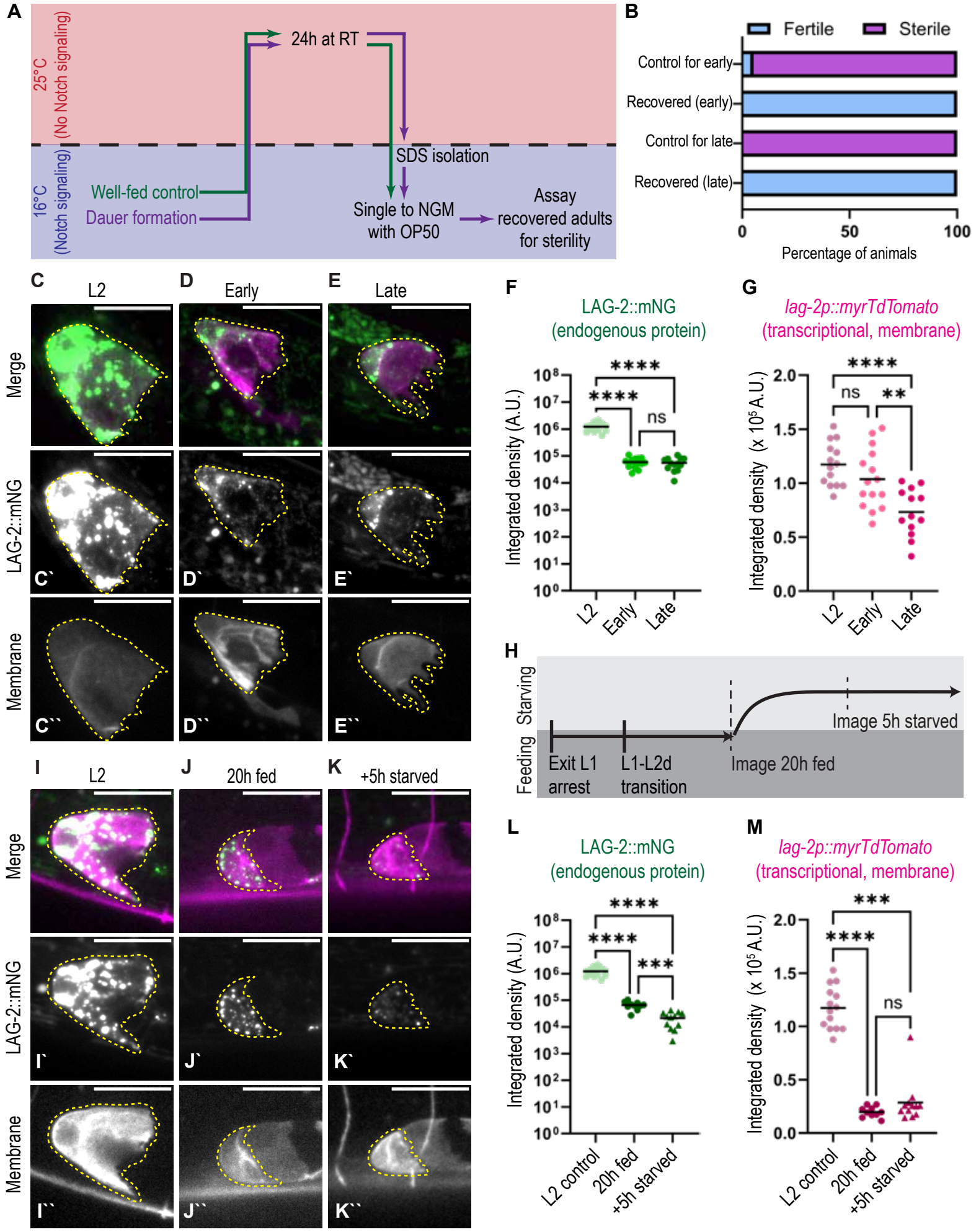
A
25°C (No Notch signaling)
16°C (Notch signaling)
24h at RT
SDS isolation
Well-fed control
Dauer formation
Single to NGM with OP50
Assay recovered adults for sterility
B
Fertile
Sterile
Control for early
Recovered (early)
Control for late
Recovered (late)
0
50
100
Percentage of animals
C L2
D Early
E Late
Merge
LAG-2::mNG
Membrane
C`
D`
E`
C``
D``
E``
F
LAG-2::mNG (endogenous protein)
Integrated density (A.U.)
****
****
ns
L2
Early
Late
G
lag-2p::myrTdTomato (transcriptional, membrane)
Integrated density (x 10^5 A.U.)
****
ns
**
H
Starving
Feeding
Image 5h starved
Exit L1 arrest
L1-L2d transition
Image 20h fed
I L2
J 20h fed
K +5h starved
I`
J`
K`
I``
J``
K``
L
LAG-2::mNG (endogenous protein)
****
****
***
L2 control
20h fed
+5h starved
M
lag-2p::myrTdTomato (transcriptional, membrane)
***
****
ns

Figure 5:

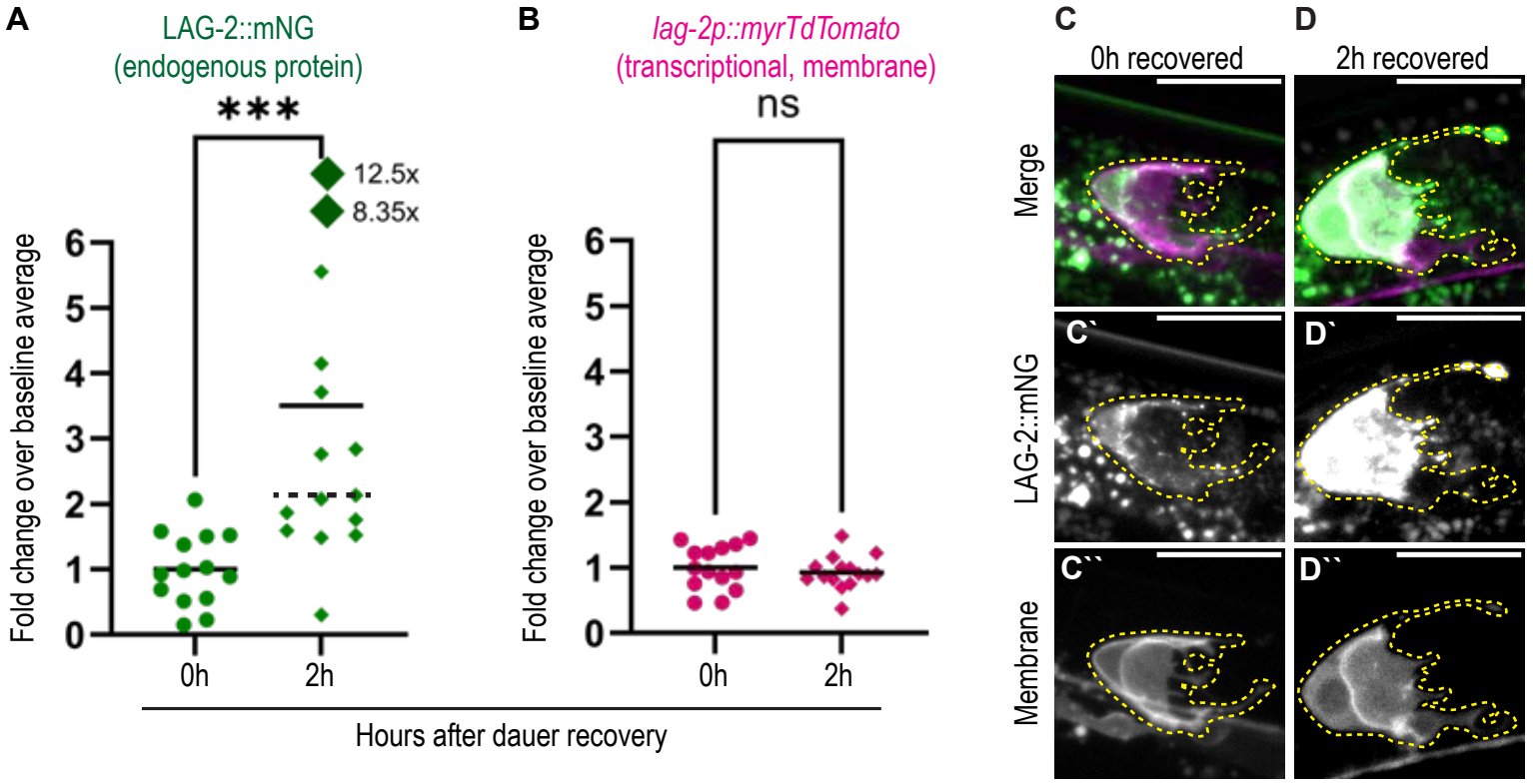
A
LAG-2::mNG
(endogenous protein)
***
12.5x
8.35x
Fold change over baseline average
0h
2h
B
lag-2p::myrTdTomato
(transcriptional, membrane)
ns
Fold change over baseline average
0h
2h
Hours after dauer recovery
C
0h recovered
D
2h recovered
Merge
LAG-2::mNG
Membrane
C`
D`
C``
D``

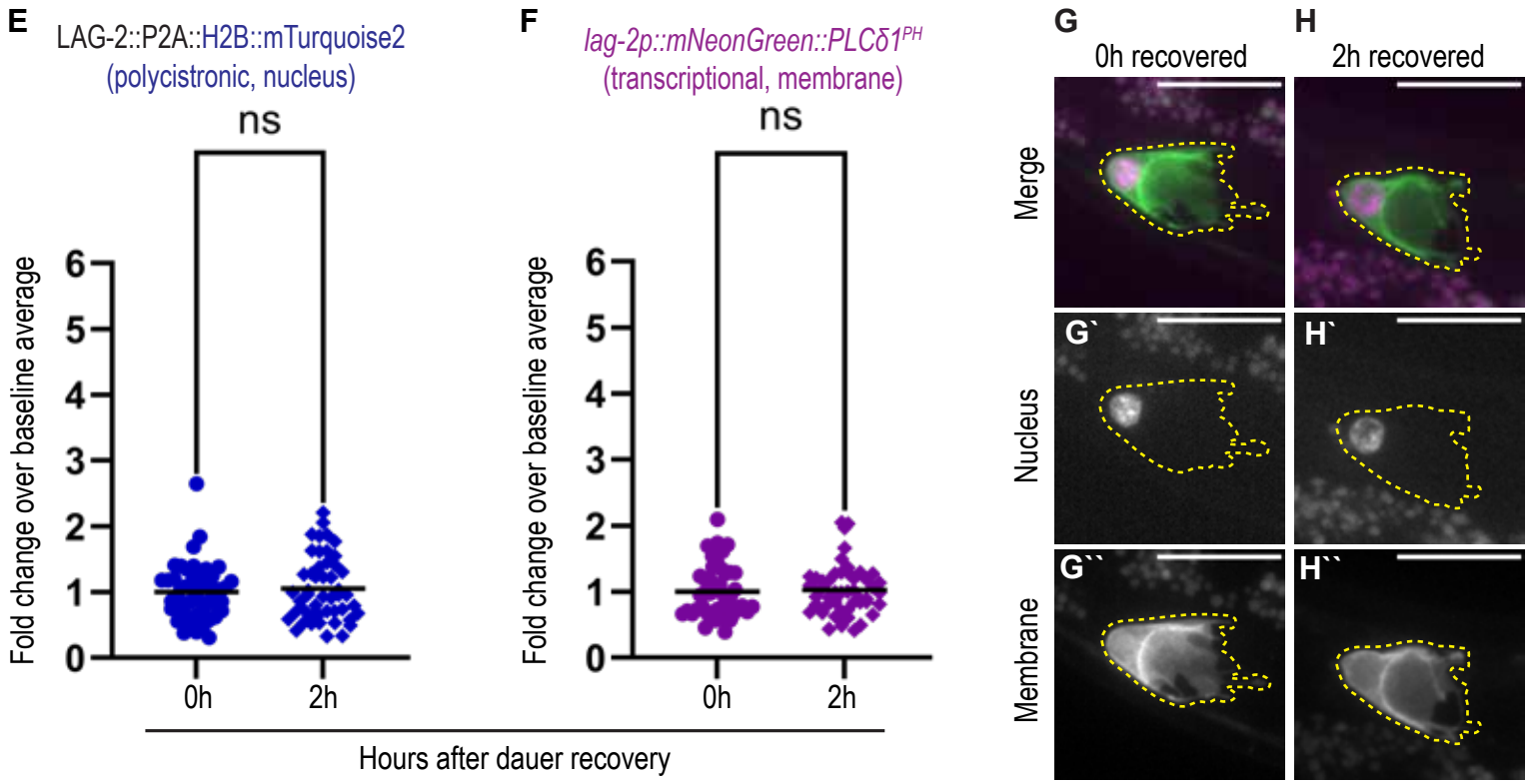
E
LAG-2::P2A::H2B::mTurquoise2
(polycistronic, nucleus)
ns
Fold change over baseline average
0h
2h
F
lag-2p::mNeonGreen::PLCδ1PH
(transcriptional, membrane)
ns
Fold change over baseline average
0h
2h
Hours after dauer recovery
G
0h recovered
H
2h recovered
Merge
Nucleus
Membrane
G`
H`
G``
H``

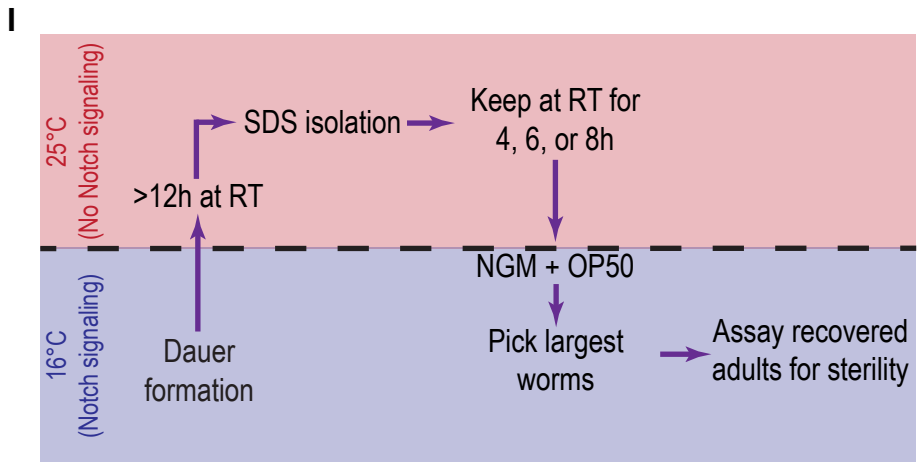
I
25°C
(No Notch signaling)
16°C
(Notch signaling)
SDS isolation
Keep at RT for
4, 6, or 8h
>12h at RT
NGM + OP50
Dauer
formation
Pick largest
worms
Assay recovered
adults for sterility

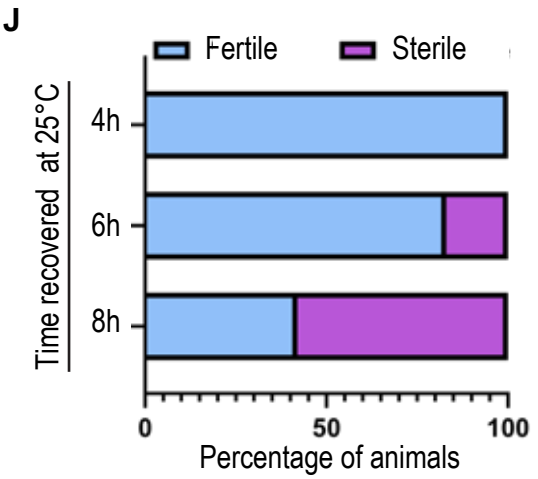
J
Fertile
Sterile
Time recovered at 25°C
4h
6h
8h
0
50
100
Percentage of animals